Centre for Archaeology Report 27/2005

Optically Stimulated Luminescence (OSL) Dating of Sands Underlying the Gravel Beach Ridges of Dungeness and Camber, Southeast England, UK

H M Roberts and A J Plater

ISSN 1473-9224

The Centre for Archaeology Report Series incorporates the former Ancient Monuments Laboratory Report Series. Copies of Ancient Monuments Laboratory Reports will continue to be available from the Centre for Archaeology (see back cover for details).

Centre for Archaeology Report 27/2005

Optically Stimulated Luminescence (OSL) Dating of Sands Underlying the Gravel Beach Ridges of Dungeness and Camber, Southeast England, UK

H M Roberts[1] and A J Plater[2]

Summary

Holocene sands underlying the gravel beach ridges of Dungeness and Camber were dated using optically stimulated luminescence (OSL) applied to coarse (sand-sized) quartz grains. The 39 sand samples dated proved sufficiently sensitive and responsive to enable well-resolved dating using the Single Aliquot Regenerative dose (SAR) measurement protocol.

The OSL chronology for the sub-gravel sands of the Dungeness foreland places the early formation of the underlying shoreface at about 5000 years ago in the region of Broomhill, with ages decreasing progressively eastwards to approximately 2000 years ago beneath Denge Marsh, and 1000-600 years ago under the present ness.

Keywords

Luminescence Dating
Geochronology

Author's address

[1] Luminescence Laboratory, Institute of Geography and Earth Sciences, University of Wales, Aberystwyth, Wales SY23 3DB. Email: hmr@aber.ac.uk

[2] Department of Geography, University of Liverpool, Roxby Building, PO Box 147, Liverpool, L69 3BX.

1. Introduction

This report describes the measurements and findings of an optically stimulated luminescence (OSL) dating study undertaken as part of a project funded by English Heritage on the late Holocene depositional history of Dungeness Foreland, and the Port of Rye.

The extensive sand and gravel beaches of Dungeness Foreland are a spectacular sedimentary monument to the long-term effects of sea-level change, storms, coastal erosion, and sediment accumulation during the Holocene period (Fig 1). They are unparalleled in the UK and are known internationally as the type-site for cuspate gravel foreland environments (May and Hansom 2003). The beaches have long attracted humans, with the oldest evidence for human activity being a group of five bronze low-flanged axes recovered from the Lydd quarry in 1985 (Needham 1988). Fire-cracked and worked flints, as well as some Bronze Age pottery, have also been identified as surface scatters on the gravel near Lydd (Barber pers comm 2002). During the Romano-British period saltworking developed as an important local industry, with saltwater trapped between the shingle beaches and evaporated over fires positioned on the higher beach crests (Barber 1998a). There follows a gap in activity until the onset of land claim from the twelfth-century AD, which continued through until the early sixteenth-century (Barber 1998b). Today, these beach deposits are attractive as a major source of aggregate for UK industry, and a long history of sand and gravel extraction has resulted in the partial destruction of the beach ridges and their associated palaeoenvironmental resource.

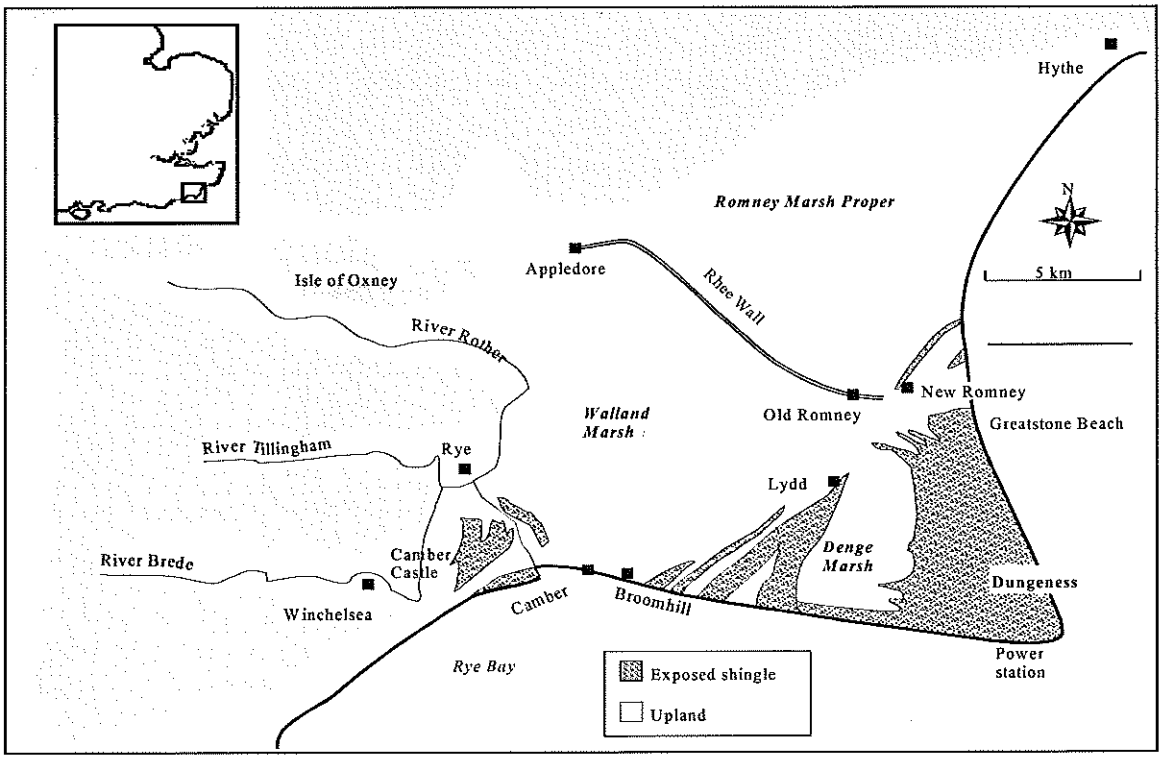

Figure 1: Dungeness Foreland and Rye.

Remarkably little is known about the age and depositional history of the 500 or so beach ridges that comprise Dungeness Foreland. Existing models suggest that the earliest beaches were in place by at least 4000 cal BP, but thereafter our chronology is reliant on limiting radiocarbon dates and archaeological finds on the gravel surface (see above), as well as palaeoenvironmental and historical records relating to the age of marshland landscapes, which abut the gravel. Consequently, we have struggled to understand how the foreland developed, and also the impacts which the evolution of the Dungeness Foreland had on the wider landscape history of the Romney Marsh depositional complex (Lewis 1932; Lewis and Balchin 1940; Eddison 1983; Long and Hughes 1995; Long and Innes 1995; Plater 1992; Plater and Long 1995; Plater *et al* 2002). The aim of the research was to establish the age, depositional origin, and landscape history of Dungeness Foreland, and to place this work in the wider setting of the Romney Marsh depositional complex, ie to develop a macroscale chronology for storms, sediment supply, and landscape change during the mid- to late-Holocene. As such, the resulting depositional history is locally important for informing models of coastal evolution and human activity, regionally significant in developing a chronology for sea-level change, storm incidence and sediment processing in the English Channel, and of wide international interest to the scientific community with an interest in the depositional history and sedimentary response of cuspate gravel forelands and their sedimentary response to environmental changes.

Amongst the project aims, optically stimulated luminescence (OSL) and palaeomagnetic secular variation (PSV) dating were used to constrain the timing of gravel deposition. These techniques were selected due to shortcomings identified in the earlier use of ^{14}C-dated material contained within the gravel complex and the minerogenic sediments both below and above. With the exception of *in situ* peat deposits which abut and overlie the gravel in the main back-barrier environment and the natural pits, respectively, these chronological data have been shown to give the age of the contained detrital organic material rather than the timing of sediment deposition. Indeed, ^{14}C dating was applied to date the most recent phase of gravel beach deposition in the region of Dungeness Nuclear Power Station (Greensmith and Gutmanis 1990), but all ages here are based on reworked sediment and many are chronologically reversed within individual boreholes. Both OSL and PSV dating have the potential to provide information on the timing of the depositional event, assuming effective bleaching on deposition in the case of OSL, or alignment of magnetic particles in the prevailing geomagnetic field during, or soon after, sedimentation in the case of PSV. Whilst this report documents the results of the OSL work, a parallel report details the PSV and environmental magnetic analyses (Plater *et al* forthcoming).

2. The principles of optically stimulated luminescence dating

Optically stimulated luminescence (OSL) dating examines the time-dependent signal that arises from the exposure of naturally occurring minerals, typically quartz and feldspar, to ionizing radiation in the natural environment. This dating technique can be applied directly to the mineral grains that make up sediment deposits, and here the event being dated is the last time the mineral grains were exposed to sunlight, ie the time the sediments were deposited and buried by further sediments. The technique relies upon the principle that any pre-existing luminescence signal contained in the sediment grains is lost on exposure to sunlight during transport, prior to deposition. Once the sediments are deposited and shielded from light exposure by the deposition of further sedimentary material, the luminescence signal re-accumulates over time through exposure to cosmic radiation, and to radiation from the decay of naturally occurring radioisotopes of uranium, thorium, and potassium located within the surrounding sediment. The luminescence signal is measured in the laboratory by stimulating small sub-samples, or aliquots, of prepared mineral grains with light – hence the term 'optically stimulated luminescence' or OSL. The size or intensity of the OSL signal observed in the laboratory is related to the time elapsed since the mineral grains were last exposed to sunlight. The OSL age is determined by calibrating the intensity of the OSL signal against known laboratory-administered radiation doses in order to determine how much radiation the sample was exposed to during burial (termed the equivalent dose, D_e, or the 'burial dose'). This value is divided by the radiation dose to which the sample was exposed each year since deposition and burial (termed the 'annual dose rate'), to give the OSL age (see Equation 1). Further details on OSL methods are given in Aitken (1998), and in recent reviews by Stokes (1999) and Duller (2004).

Equation 1

$$\text{OSL age (years)} = \frac{\text{Burial dose (Grays)}}{\text{Annual dose rate (Grays per year)}}$$

(1 Gray = 1 Joule/kg)

In this study, the D_e was obtained using the Single Aliquot Regenerative dose (SAR) measurement protocol (Murray and Wintle 2000), applied to coarse-grained quartz (ie grains > 90μm diameter). Working with quartz offers the advantage that it is not subject to anomalous fading, unlike some feldspars (eg Spooner 1994; Huntley and Lamothe 2001). The SAR protocol uses the response to a fixed test dose to correct for any change in luminescence sensitivity occurring in the sample during laboratory measurements (eg as a result of thermal pretreatments), with all of the measurements necessary for the determination of D_e being made on a single aliquot. By measuring several aliquots, many independent determinations of D_e can therefore be obtained. Figure 2 illustrates how D_e is obtained from the SAR measurements made. Following measurement of the natural luminescence intensity (denoted by the square symbol on the y-axis of Fig 2), the response (L_x) to a series of artificial

radiation doses is measured, and normalised to the response (T_x) to a fixed test dose. A normalised dose-response or 'growth' curve can then be constructed by plotting the ratio L_x/T_x as a function of radiation dose. This enables the natural luminescence intensity to be calibrated to these responses to a given laboratory radiation dose, thereby determining the laboratory equivalent dose, D_e.

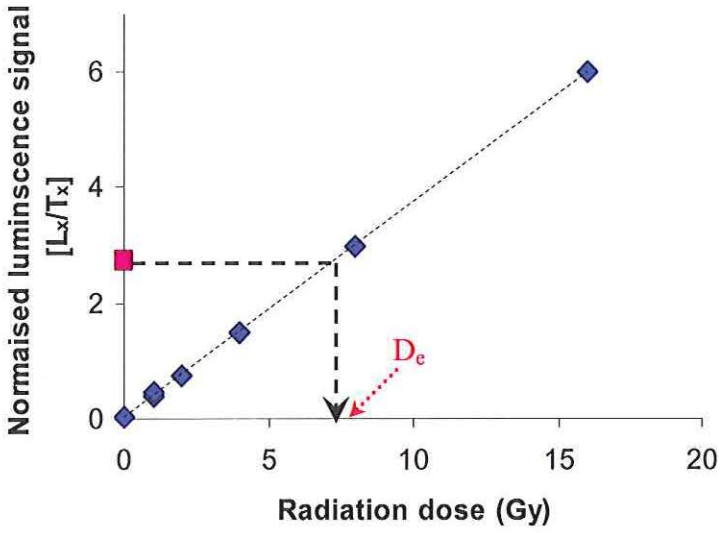

Figure 2: Dose-response or 'growth' curve (diamond symbols) generated from measurements made using the Single Aliquot Regenerative dose (SAR) measurement protocol, used in this study. The natural luminescence intensity (square symbol) of the aliquot is calibrated against the response to these known artificial irradiation doses to determine the laboratory equivalent dose, D_e.

3. Sample sites and OSL sample collection

In this project, OSL dating was to be used to date the sands underlying the gravel beach ridges of Dungeness and Camber. A series of 13 boreholes were drilled through the gravel beaches and into the underlying sands, by *Strata Investigation Services*. Figure 3 shows the location of the 13 boreholes, whilst Table 1 gives details of the map reference for each core and the altitude of the surface of each core. The boreholes were cased with a steel liner through the gravel, to prevent backfilling, and then a 38mm diameter plastic-lined steel sampling chamber was percussion driven into the sands to sample them. Successive 1m depths of sand were sampled, and each plastic core-tube liner section was sealed prior to transport to the laboratory. In addition, a sample was taken from a sand unit at Moneypenny Farm using a 60cm length of 7cm diameter opaque plastic pipe driven into the base of a pit, deepened by hand to approximately 2m depth. The location of this sample site is also shown on Figure 3.

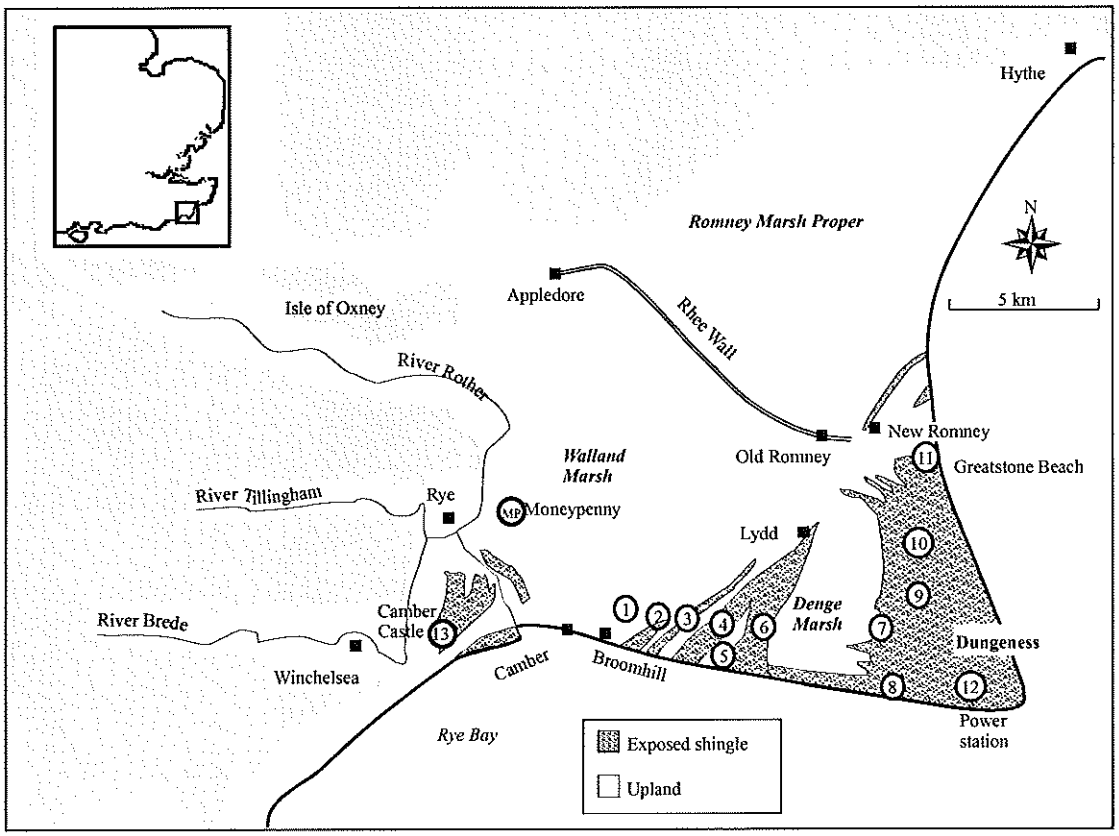

Figure 3: Core locations from which OSL samples were collected

Table 1: Location and altitude of OSL cores taken for this study of Dungeness and Rye.

Dungeness deep drill sites

OSL sample prefix is: '*Aber*-73BH-'

Site No.	Location	Grid ref	m OD
1	Broomhill Farm	TQ 99207 19691	2.86
2	The Midrips (Belfast)	TQ 99669 18388	4.26
3	The Forelands	TR 01155 18696	4.43
4	Holmstone	TR 02383 18560	4.49
5	South Brooks	TR 02761 17859	3.45
6	Dungeness Road Gate	TR 03865 18410	4.29
7	Dengemarsh Road (pylons)	TR 05669 17849	4.14
8	Dungeness Lookout	TR 06368 16922	5.16
9	RSPB Visitor Centre	TR 06859 19043	3.13
10	ARC	TR 06831 20014	3.91
11	Greatstone	TR 07732 22423	3.05
12	Power Station	TR 08099 17155	5.55
13	Castle Farm (Rye project)	TR 91986 17631	4.53

Moneypenny farm hand-cored site

OSL sample prefix is: '*Aber*-80MP-'

Site no.	Location	Grid ref	m OD
1	Moneypenny Farm	TQ 9509 2080	3.87

To check the efficacy of bleaching in this environment, two surface samples were taken from Greatstone Beach, namely from the upper shoreface sands and from symmetrical sand ripples observed on the beach. These 'modern' samples represent a present day analogue for the environment of deposition of the OSL samples, and should give an age of zero years, within errors, if the samples are well bleached at the time of deposition.

Three samples were taken from 12 of the 13 deep-drill cores for preparation prior to OSL dating; core number 5 was relatively short in length, therefore only 2 samples were taken (see Figs 4 and 5). Care was taken to ensure that all samples were selected from homogeneous units and at ≥30cm from any change in stratigraphic unit, to avoid potential complications from any differences in dosimetry (30cm being the approximate distance of effective gamma radiation from ^{40}K: Aitken 1994). One sample from the short, hand-retrieved core from Moneypenny Farm, plus the two modern samples from Greatstone beach, were also taken for laboratory preparation. A total of 41 samples was selected and prepared for OSL dating.

The laboratory codes assigned to the 13 Dungeness and Rye borehole cores are prefixed by '*Aber*-73BH' followed by the borehole number. The sample taken from Moneypenny farm has the code '*Aber*-80MP-1', and the modern samples from Greatstone beach use the following codes: '*Aber*-73BH-USS' – upper shoreface sands, and '*Aber*-73BH-SSR' – symmetrical sand ripples.

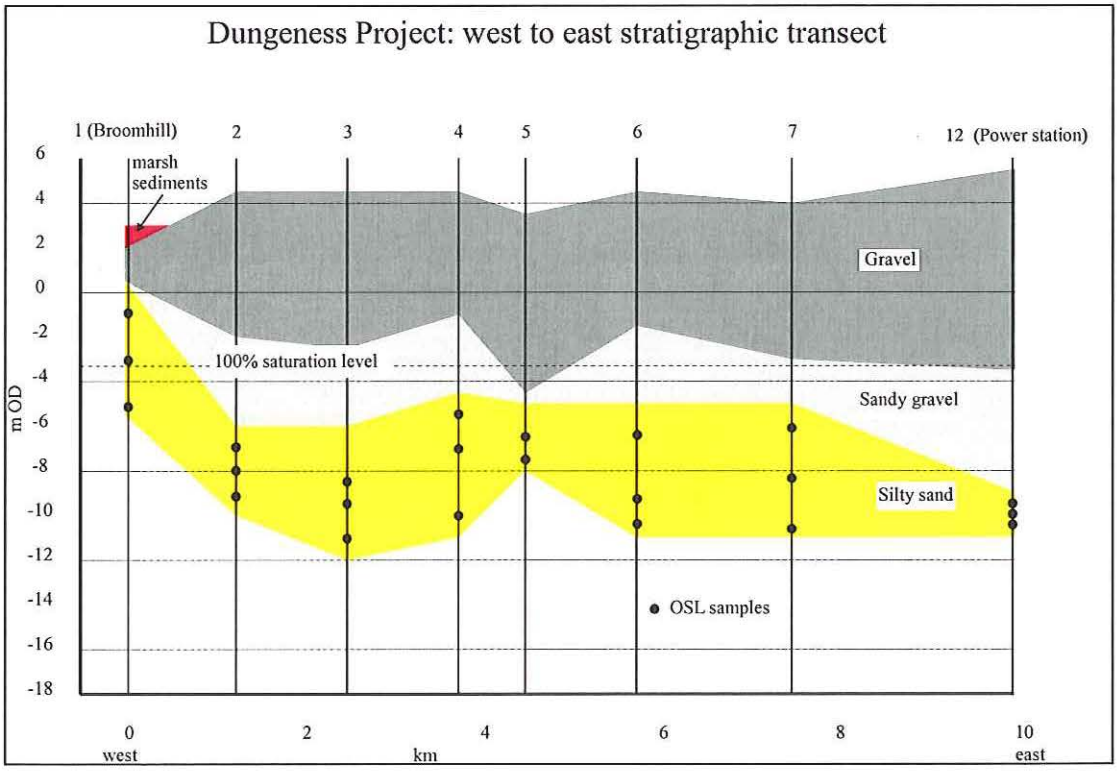

Figure 4: West to east stratigraphic transect across Dungeness Foreland showing boreholes drilled for OSL dating and the depths of OSL samples. The 100% saturation level at 3000 years ago is also shown as a horizontal dotted line (see section 6 for further discussion).

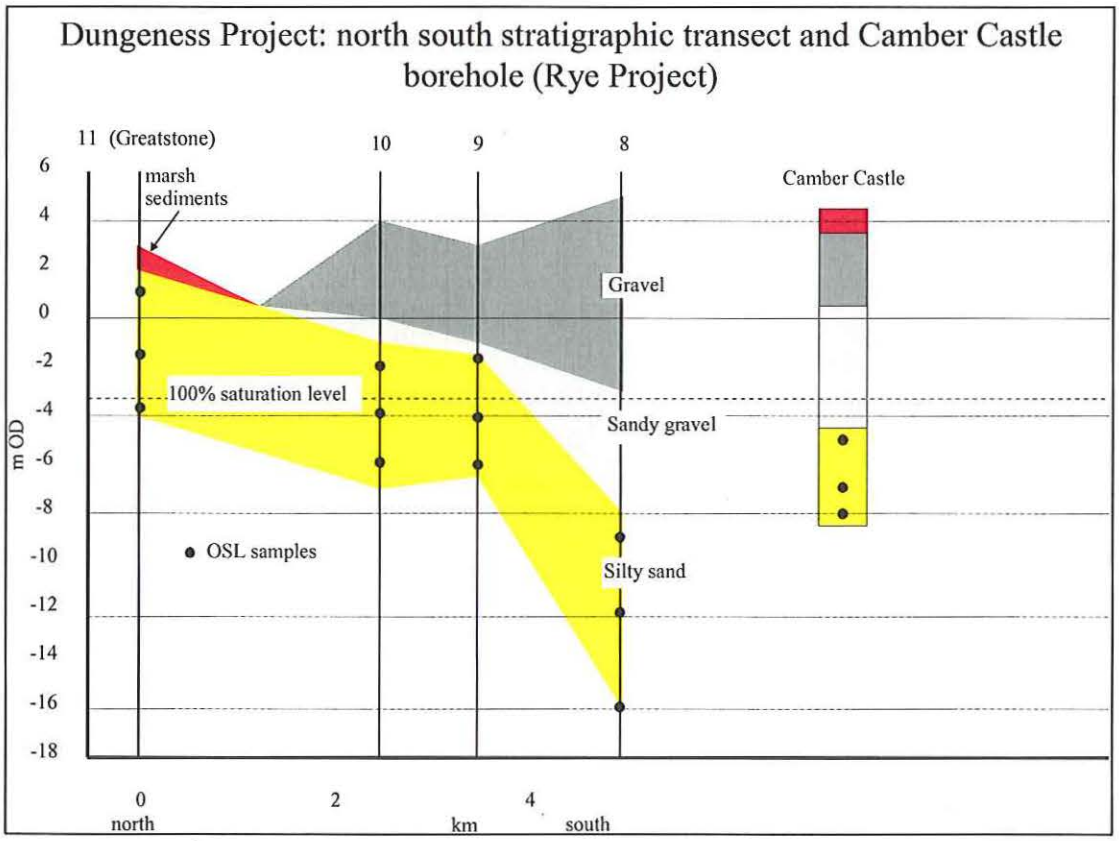

Figure 5: North to south stratigraphic transect across Dungeness Foreland showing boreholes drilled for OSL dating and the depths of OSL samples. The 100% saturation level at 3000 years ago is also shown as a horizontal dotted line (see section 6 for further discussion).

4. OSL sample preparation

Samples were taken for preparation for OSL measurements by gently hand-sawing through the plastic core liner at the appropriate depth under subdued red lighting conditions in the luminescence laboratory. The core-liner used to obtain the sand cores was made of transparent plastic, hence the outer portion of the core that had been exposed to daylight during sampling and core retrieval had to be removed prior to further processing for luminescence dating. This was achieved by driving a 20mm diameter thin-walled cylindrical corer of 100mm length, down through the centre of the 38mm diameter sand core at the appropriate sample depth, to retrieve material suitable for luminescence dating that had not been exposed to daylight during sampling. This inner 20mm diameter portion of the core was taken for preparation of coarse-grained quartz, using standard methods, outlined below.

Samples were pre-treated with a 10% v.v. dilution of concentrated (37%) hydrochloric acid (HCl) to remove carbonates and surficial coatings, then washed three times in distilled water. Samples were then treated with 20 vols. hydrogen peroxide (H_2O_2) to remove organic material, and then washed as previously. Samples were dried and then sieved using the following mesh sizes: 355, 300, 250, 212, 180, 150, 125, 90 micron diameter mesh. The modal grain size for each sample was typically selected for further processing prior to OSL dating. In two cases, namely core 1 and core 10, two grain sizes were selected for further processing, to investigate the age determined for each of those grain sizes.

The grain sizes selected for OSL dating were refined using a solution of sodium polytungstate ('heavy liquid') to separate out the quartz material from the feldspar and heavy mineral fractions of the sediments, on the basis of differences in density. The quartz-rich fraction of the sediments (density between 2.62 – 2.70 gcm^{-3}), was treated with 40% hydrofluoric acid (HF) for 45 minutes, to remove the alpha-irradiated surface of the quartz grains and to dissolve any remaining feldspar material, followed by a further 45 minutes in concentrated (37%) HCl, to dissolve any fluorides formed during the etch procedure. The samples were rinsed a minimum of 3 times in distilled water, centrifuging between washings, and then dried at 50°C, prior to re-sieving. This final sieving acts as a further quartz purification step, as it removes feldspar grains which have not been totally dissolved with HF, but which have been significantly etched and therefore reduced in diameter. The final quartz is then ready for OSL measurements to determine the 'burial dose' or equivalent dose, D_e.

The outer, light-exposed material removed from around each OSL core sample was suitable for laboratory-based measurements of water content and dosimetry as these measurements do not require un-exposed sample material. The cores had been sealed immediately on sampling and were stored horizontally, thus preserving their water content. The outer, light-exposed portion of each OSL sample was weighed prior to drying at 50°C. Drying continued until a constant mass was recorded, to establish the field

water content at the time of sampling. Little compaction had been observed in the cores on sampling, as is typical of percussion-cores (Ridgway *et al* 2000), hence no correction was required for this. The water content values employed in the final age calculations are discussed more fully later in section 6, however these measurements of conditions at the time of sampling provide a benchmark for calculations which follow later. After drying, the light-exposed material was then crushed to a fine powder using a ball mill, prior to thick source alpha and beta counting (discussed further below, section 5) to determine the annual dose rate to the sample.

5. Equipment and Methods

All OSL measurements were conducted using an automated *Risø* TL/OSL reader, equipped with a combined high-power blue LED/ infra-red laser diode OSL unit, and a beta source for irradiations. The combined OSL unit was employed at 80% of full diode current, providing approximately 17mW/cm^2 power from the blue LED unit (470nm), and 370mW/cm^2 from the IR laser diode (830nm). All measurements were made whilst holding the sample at 125°C, and OSL was detected using 7.5 mm Hoya U-340 filters.

Measurements of OSL were made on coarse-grained quartz, using the Single-Aliquot Regenerative-dose (SAR) protocol of Murray and Wintle (2000). The advantage of SAR over previous measurement protocols is that it uses a measurement of the luminescence production per unit dose to monitor and correct for changes in luminescence sensitivity that have occurred as a function of time, temperature, and past-radiation exposure (Wintle and Murray 2000). The SAR procedure permits the determination of an equivalent dose (D_e), and hence potentially an OSL age, for each aliquot examined.

As part of the sequence of OSL measurements made, outlined in Table 2, a minimum of three regenerative beta doses were applied to each aliquot, bracketing the expected natural dose. Two zero beta doses were included towards the beginning and end of the measurement cycle to monitor recuperation, and the first regenerative dose (applied at the end of the measurement protocol) was repeated to monitor the sensitivity correction applied (this is sometimes referred to as monitoring of the 'recycling'). Following measurement of each natural or regenerative-dose signal, a fixed test dose was applied, with a cut-heat of 160°C, to monitor and correct for sensitivity change during the measurement procedure. Measurements were made for a range of pre-heat temperatures (held for 10s) to enable D_e to be obtained as a function of pre-heat temperature: either 160-300°C in 20°C step intervals, with 3 aliquots at each temperature, where a minimum of 24 aliquots were employed in a dating run, or 160-280°C, with 3 aliquots at each temperature, where 21 were employed.

Table 2: Outline of the SAR measurement protocol. A minimum of three regenerative doses were employed in this study, designed to bracket the natural signal.

Step Number	SAR sequence description
1	Preheat: (160-300°C), heating rate 5°C/s, hold at temperature for 10s
2	Measure natural or regenerative dose signal ('L_x'): 100s OSL @125°C
3	ApplyTest Dose
4	Cut heat: 160°C, heating rate 5°C/s
5	Measure test dose signal ('T_x'):100s OSL @125°C
6	Apply 0Gy dose ('recuperation' check)
7-11	*Repeat steps 1-5*
12	Apply regenerative dose 1
13-17	*Repeat steps 1-5*
18	Apply regenerative dose 2 (larger than dose 1)
19-23	*Repeat steps 1-5*
24	Apply regenerative dose 3 (larger than dose 2)
25-29	*Repeat steps 1-5*
30	Apply 0Gy dose ('recuperation' check)
31-35	*Repeat steps 1-5*
36	Apply regenerative dose 1 ('recycling' test)
37-41	*Repeat steps 1-5*

Dose-rates were determined using *Daybreak* detectors for thick source alpha counting and a *Risø GM-25-5* beta counter for beta counting, applied to finely ground bulk sample material. The depth and method of sampling precluded the use of a field gamma detector. The gamma dose-rate was estimated using the uranium and thorium determinations from the pair count and calculated potassium contents. The latter were derived by subtraction using the measured beta dose-rate and that calculated from the uranium and thorium values. The cosmic ray dose was estimated from the burial depth (Prescott and Hutton 1994). Water contents were determined in the laboratory from sealed field samples (section 4), and the values employed in the calculation of ages are discussed further in section 6. Moisture and beta attenuation factors are given in Aitken (1985). The alpha and beta counting results, cosmic dose rates, water content values, and the dose rates calculated using the conversion factors of Adamiec and Aitken (1998), are given for each sample in the final age tables (Tables 7.1 – 7.15).

6. Assessment of the water content

An assessment must be made of the past and present variability of water content for each sample, as water in the sediments attenuates naturally occurring radiation, reducing the effective dose rate to the sediment grains. Measurements were made in the laboratory of the field water content of each OSL sample (described in section 4), given in Table 3. The field determinations of water content for the deep drill cores (73BH 1-13) are thought to reflect the conditions in the sub-gravel sands at the time of sampling fairly accurately, for three reasons: 1) little compaction was observed on sampling, 2) cores were taken using percussion rather than vibration, thereby minimising dewatering, and 3) the water pressure had to be maintained during sampling of the sub-gravel sands to prevent the sediment from boiling. These measurements of field water content helped to provide a benchmark figure for the water content at the time of sampling (25 ± 5%), however, what is important to assess is the water content history of each sample for the whole of the time period from deposition until the time of sampling. Any assessment of the water content should take into account both seasonal- and longer-term fluctuations, and on-site discussions with geomorphologists with knowledge of the palaeoenvironmental conditions are of critical importance to determine the fraction of saturation (ie a value reflecting the wetting and drying of the sediments over the time since deposition).

In discussion with Dr AJ Plater and Dr P Stupples of the University of Liverpool, a model was developed to reconstruct the fraction of saturation and water content history of each sample in the Dungeness and Rye projects, and hence to determine a value for water content, which represents the whole of the depositional period. This model is based on observations of pore water content and interstitial drainage characteristics of sediments in the present inter- to supratidal zone. This is coupled with an estimation of altitudinal change in tidal level, with no overall change in tidal dynamics, during the likely period of sediment deposition, ie the late Holocene (4000-3000 years BP) to present. The model is shown below (Fig 6), and discussed in sections 6.1 - 6.3; the final water content values employed in the age determinations are given for each sample in the final age tables (Tables 7.1 – 7.15).

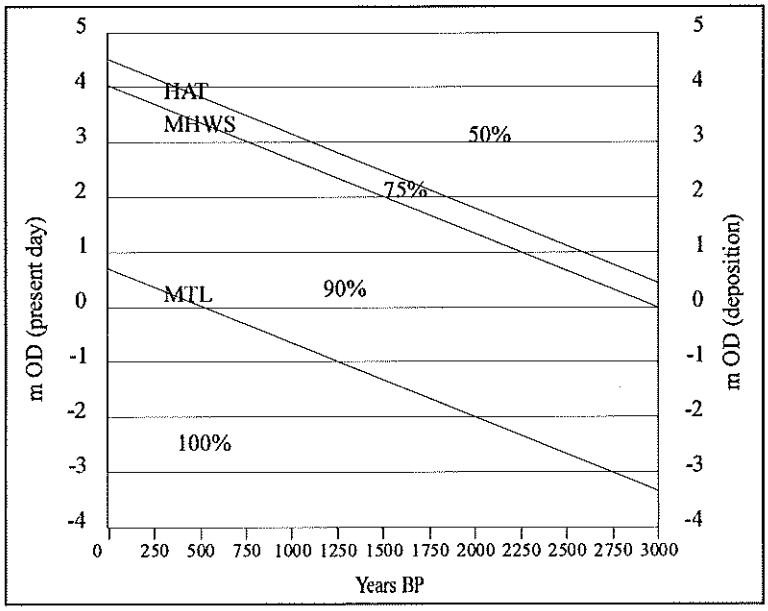

Figure 6: Fraction of saturation history model for late Holocene inter- and supratidal sand samples from Dungeness and Rye. Inclined zone boundaries are a function of long-term changes in tidal level due to relative sea-level rise.

Table 3: Measured field water content values (expressed as a percentage of the mass of dry sediment). For reasons discussed in section 6, the deep drill cores (73BH 1-13) are believed to reflect conditions at the time of sampling quite accurately. The average as-sampled water content calculated for all of the OSL dating samples below is 22 ± 3%. Based on the tabulated values, a slightly broader common value of 25 ± 5% was used as a benchmark water content for all 39 dating samples, prior to correction using the fraction of saturation model discussed in sections 6.1-6.3.

Sample	% water content
73BH-1/1	19.9
73BH-1/2	23.5
73BH-1/3	11.7
73BH-2/1	19.9
73BH-2/2	21.6
73BH-2/3	22.0
73BH-3/1	21.8
73BH-3/2	24.3
73BH-3/3	23.2
73BH-4/1	20.8
73BH-4/2	21.3
73BH-4/3	24.3
73BH-5/1	22.6
73BH-5/2	22.7
73BH-6/1	22.7
73BH-6/2	23.8
73BH-6/3	23.1
73BH-7/1	33.4
73BH-7/2	22.7
72BH-7/3	24.0
73BH-8/1	22.0
73BH-8/2	20.2
73BH-8/3	24.5
73BH-9/1	23.6
73BH-9/2	24.6
73BH-9/3	22.6
73BH-10/1	21.7
73BH-10/2	21.8
73BH-10/3	22.5
73BH-11/1	23.7
73BH-11/2	13.6
73BH-11/3	24.2
73BH-12/1	19.3
73BH-12/2	21.8
73BH-12/3	20.8
73BH-13/1	24.9
73BH-13/2	22.9
73BH-13/3	23.5
80MP-1	16.2

6.1 Inter- and supratidal water content and drainage

The tidal levels of relevance to our model are mean tidal level (MTL), mean high water of spring tides (MHWS), and highest astronomical tide (HAT). The present altitudes of each datum at Dungeness are expressed on the left-hand vertical axis of the model (Fig 6), namely +0.68, +4.03, and +4.50m OD, respectively. For sites of deposition below MTL, a fraction of saturation value of 100% is assumed. Here, not only are all interstitial spaces filled with water, ie saturated, but any drainage occurring during the low tide phase is compensated by the movement of water into these interstices from the upper part of the tidal flat. Hence, there is no overall change in this 100% saturation level during the tidal cycle.

For sites on the tidal flat between MTL and MHWS, saturation is again achieved during the tidal cycle, ie 3-4 hours either side of high tide, but in this case drainage of interstices during the low tide phase is not fully compensated by the supply of water draining from higher on the tidal flat (and above). In this case, an average saturation value of 90% reflects the fact that 100% saturation is not maintained during the low tide phase, and that the period of time during which saturation prevails decreases towards MHWS.

The effect of interstitial drainage during the low tide phase becomes more pronounced with altitude. Hence, the zone between MHWS and HAT may well achieve saturation for a reasonable period of time during the high tide phase but the period for interstitial drainage is considerably longer. In addition, the water content in the sediments found towards the upper part of this zone can only be maintained by freshwater drainage from the regional watertable for much of the year. Therefore, the average 75% value for the fraction of saturation reflects a general pore water content that can achieve saturation at best, but is usually less than maximum. In addition, such a near-saturation water content cannot be maintained during the tidal cycle.

The last of the altitudinal zones is that above HAT. Sediments in this zone are beyond the reach of the tide but generally lie within the influence of the fresh watertable. Whilst high water contents, ie near-saturation, may be achieved during the winter when the regional watertable becomes elevated, the sediments may become dry (depending on altitude relative to the watertable height) during the summer. In this case, a fraction of saturation value of 50% reflects this annual variability.

The combination of maximum and minimum estimated fraction of saturation values with temporal variability (a) during the tidal cycle and (b) during the year, therefore, defines the zonal fraction of saturation values outlined in the model.

6.2 Sea-level change

Whilst acknowledging the estimates of fraction of saturation and water content history relative to the regional watertable, an additional parameter is relative sea-level rise during the late Holocene. This period not only witnessed the

growth of Dungeness Foreland and the back-barrier marshland but also experienced a rise in tidal level associated with relative sea-level rise, ie a combination of global eustatic rise coupled with local- to regional-scale crustal movement. As a consequence, the fraction of saturation and water content history of the sediments will have changed in response to relative sea-level rise during the late Holocene, ie the estimated period of time since deposition of the foreland began.

A clear chronostratigraphic marker for the altitude of former tidal levels in the region of Dungeness is the upper surface of the main marsh peat bed, which is present across Walland Marsh (Long and Innes 1995). This is found at an altitude of approximately 0m OD and dates from *c* 1200 cal BC (*c* 3000 BP). According to the stratigraphic methodology used to reconstruct Holocene sea-level trends (Shennan 1986), the transition from a monocotyledonous peat to an overlying saltmarsh deposit takes place at approximately MHWS at the time of deposition. Hence, the altitude of MHWS at *c* 1200 cal BC (*c* 3000 BP) can be assumed to be *c* 0m OD. If no change in tidal dynamics is assumed for this period, ie tidal range has remained constant, then MTL, MHWS and HAT may all be reduced by 4.03m to give their altitudes *c* 3000 years ago. Although palaeotidal change does occur as a consequence of changing water depth and coastal morphology, the majority of change in tidal range in the English Channel region was probably achieved following the opening of the Straits of Dover at *c* 7050 cal BC (*c* 8000 BP; Austin 1991). Indeed, in the North Sea, Shennan *et al* (2000) have illustrated that significant increases in tidal range due to sea-level rise were complete by *c* 4900 cal BC (*c* 6000 BP). However, this largely discounts any impact resulting from the infilling of large estuaries and embayments which, in the case of The Wash and the Humber, has been shown to increase tidal range by *c* 2m during the mid- to late Holocene (Shennan and Horton 2002).

Although the water content model needs to be capable of reconstructing the fraction of saturation and water content history for sediments older than 3000 years, earlier unequivocal chronostratigraphic markers or waypoints of tidal level are not so clearly identified or readily available in the region of Dungeness. Hence, a linear trend line has been constructed from the present day to *c* 1200 cal BC (*c* 3000 BP), beyond which further linear interpolation is adopted. This is based on the absence of any significant change in the rate of sea-level rise in the Romney Marsh region during the last 5000 years or so (eg Spencer *et al* 1998a).

Both past and present tidal levels are given on their respective right- and left-hand vertical axes of the water content model (Fig 6). The zonal fraction of saturation and water content history described above is then applied to the areas enclosed by the inclined zone boundaries, illustrating how both the fraction of saturation and temporal variability in this water content will have changed over the long-term in response to relative sea-level rise.

6.3 Calculating water content and water content history

From the model described above and shown in Figure 6, calculating the combined fraction of saturation and water content history for any given sediment sample is a matter of first reading the sample age, calculated using the measured field water content value, along the horizontal axis of the graph, and identifying sample altitude on the vertical axes. Reading from left to right then gives the period of time the sample has spent in each of the defined water content zones. For example, a sample from *c* +1.0m OD assumed to be 3000 years old will have experienced the following:

0–2250 years ago (2250 years) at 90% saturation = (2250/3000) x 90% = 67.5%
2250–2600 years ago (350 years) at 75% saturation= (350/3000) x 75% = 8.75%
2600-3000 years ago (400 years) at 50% saturation= (400/3000) x 50% = 6.67%
Σ = 83%

The average fraction of saturation value for the sample is then determined by dividing the number of years within a water content zone by the total number of years, and then multiplying by the zonal fraction of saturation values. The sum of these zonal periods then gives the average fraction of saturation for the period since deposition. For the above example, this is approximately 83%. This value is combined with the water content based on the field values (25 ± 5%), to give a water content for use in the calculation of the luminescence age of 21% (expressed as % dry mass of sediment).

The OSL age can then be recalculated based on the revised estimate of water content, which includes water content history (ie 21%), and the re-calculated age can then be used to relocate the sample on the water content history graph (Fig 6). In the case of the above, if the re-calculated OSL age was 2500 years, the water content history would be recalculated as follows:

0–2250 years ago (2250 years) at 90% saturation = (2250/2500) x 90% = 81.0%
2250–2500 years ago (250 years) at 75% saturation= (250/2500) x 75% = 7.5%
Σ = 89%

This procedure is continued iteratively until the calculated OSL age is unchanged from the previous calculation after an iteration. In practice, a maximum of one iteration was necessary for any sample in this study because the effect on the age was not as great as the 500 year shift in age shown in the hypothetical example. For samples where the age is greater than 3000 years, the inclined zone boundaries and the corresponding zonal water contents are extrapolated linearly.

With the exception of six samples from Dungeness and one from Moneypenny Farm (Rye project) all other samples lie below –3.35m OD and have, therefore, experienced 100% saturation water content for the last 3000 years. Due to the young nature of three of these samples from Dungeness (namely, samples *Aber*-73BH-9/1, -10/1, and -11/2), they fall within the 100% saturation zone from the time of deposition until present. Only samples *Aber*-73BH-11/1, -1/1, and -1/2, plus sample *Aber*-80MP-1 from Moneypenny farm, required

further consideration of their water content. The water contents used for final age determinations are presented in the final age tables (Tables 7.1 – 7.15).

7. Results of experimental checks

As part of the OSL measurements made in this project, a series of checks were undertaken to monitor the OSL measurement procedure, the response and behaviour of the samples, plus the choice of grain size and aliquot size. These experimental checks are discussed below.

7.1 Grain size

In this study, the samples were sieved using a mechanical shaker and a range of mesh sizes (see section 4), and typically the modal grain size was selected for further processing prior to OSL measurements for the determination of the burial dose, or the equivalent dose, D_e. The calculation of the dose rate for use in the determination of an OSL age takes into account the grain size (Bell 1979; Mejdahl 1979). The grain size selected for the majority of samples was 150-180μm, although 125-150μm and 180-212μm were also used in this study. The grain size used for dating is listed for each sample in the final OSL age tables (Tables 7.1 – 7.15).

Two samples (*Aber*-73BH-1/1 and *Aber*-73BH-10/3) selected at random were examined using two different grain sizes, to check that there were no differences in the final ages calculated. Sample *Aber*-73BH-1/1 was examined using 150-180μm and 180-212μm grain sizes. These two grain sizes gave final ages which agreed within errors, being 4810 ± 180 years for 150-180μm grains (based on 31 aliquots) and 4980 ± 190 years for 180-212μm grains (n=40 aliquots). The two grain sizes examined for sample *Aber*-73BH-10/3 also gave ages which agreed within errors, being 1060 ± 40 years for 125-150μm and 1030 ± 50 years for 150-180μm. Use of different grain sizes for various samples in this study does not, therefore, appear to present any problem for these samples.

7.2 Aliquot size

Prepared quartz grains for each sample were presented for OSL measurements by mounting the grains in a monolayer onto 1cm diameter aluminium discs, sprayed lightly with Silkospray™ silicone oil to hold the grains in place during measurement. The discs, or aliquots, may be prepared using various amounts of sample. Looking at large aliquots (8mm diameter, giving ~500 grains per aliquot) maximises the luminescence signal observed from each aliquot, which may be useful where signal levels are low due to insensitive material or where young samples are being examined. Medium aliquots (5mm diameter, giving ~200 grains per aliquot), and small aliquots (2mm diameter, giving ~30 grains per aliquot), allow the study of fewer grains, which increases the possibility of identifying incompletely bleached samples because for a sample with non-homogenous D_e, the scatter in D_e values

should increase as the number of grains per aliquot decreases (Olley *et al* 1999).

In this study, medium-sized aliquots were examined wherever possible, with large aliquots being examined in cases where signal levels were seen to be low due to the young age of the samples and/or a lack of sensitivity of the material. Seven samples, selected at random, were examined using both medium and large sized aliquots prepared from the same quartz grain size, to examine any effect of changing aliquot size on the determination of D_e. The D_e values determined for the medium and large aliquots are given in Table 4, and for each of the seven samples (including one at two grain sizes) the D_e values determined for the different aliquot sizes agree within errors (2σ error for 73BH-10/2 and -11/1, 1σ for the remaining 6 samples examined). Aliquot size is not, therefore, an important factor in the determination of D_e for this study.

Table 4: Comparison of D_e values obtained for medium and large aliquots for samples selected at random from this study. The number of aliquots considered in each D_e determination is also given, in brackets.

Sample	Mean D_e of medium aliquots (Gy)	Mean D_e of large aliquots (Gy)
Aber-73BH-1/1 150-180μm	3.68 ± 0.08 (n=15)	3.73 ± 0.08 (n=16)
Aber-73BH-1/1 180-212μm	3.76 ± 0.08 (n=19)	3.83 ± 0.10 (n=21)
Aber-73BH-1/2	3.12 ± 0.06 (n=16)	3.10 ± 0.06 (n=17)
Aber-73BH-7/3	1.21 ± 0.04 (n=15)	1.19 ± 0.03 (n=14)
Aber-73BH-10/1	0.56 ± 0.02 (n=14)	0.57 ± 0.02 (n=15)
Aber-73BH-10/2	0.76 ± 0.02 (n=15)	0.68 ± 0.02 (n=13)
Aber-73BH-11/1	0.38 ± 0.02 (n=17)	0.33 ± 0.01 (n=18)
Aber-73BH-12/1	0.51 ± 0.02 (n=14)	0.51 ± 0.07 (n=18)

7.3 OSL signal checks

The OSL signal of each aliquot measured was examined visually, to check the initial signal intensity and the form of the decay curve. A typical decay curve is

shown in Figure 7, and shows a rapid decrease in signal, which is characteristic of the decay of a signal from quartz. Routinely, the D_e values were calculated using the first two data channels (0.8 s stimulation) and the background was taken from the end of the decay curve (channels 230-250, the final 8.4 s stimulation). This maximised the contribution of the fast component of the OSL signal (Bailey *et al* 1997; Murray and Wintle 2003), and typically represented ~15-25 % of the total OSL signal.

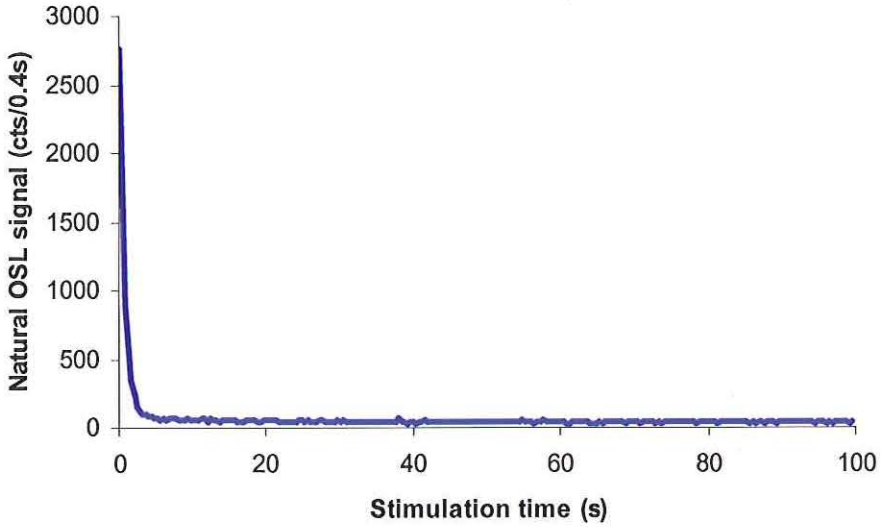

Figure 7: Typical OSL signal for aliquots in this study. The example shown is from an aliquot of sample 73BH-1/1, which was preheated to 220°C/10s. The very rapid decrease in signal, quickly reaching a steady low background is a form which is frequently observed in the study of quartz aliquots. The signal integrated to derive the value of D_e is that from the first 0.8s of optical stimulation.

The form of the dose-response or 'growth' curve was also examined, and a minimum of three artificial irradiation doses were used to define the growth curve for each aliquot, designed to bracket the 'natural' signal and hence determine the value of D_e. Figure 8 shows a typical growth curve; error bars are shown, calculated following Banerjee *et al* (2000) and Galbraith (2002), and generated by *Analyst* (written by Dr. Geoff Duller, University of Wales, Aberystwyth).

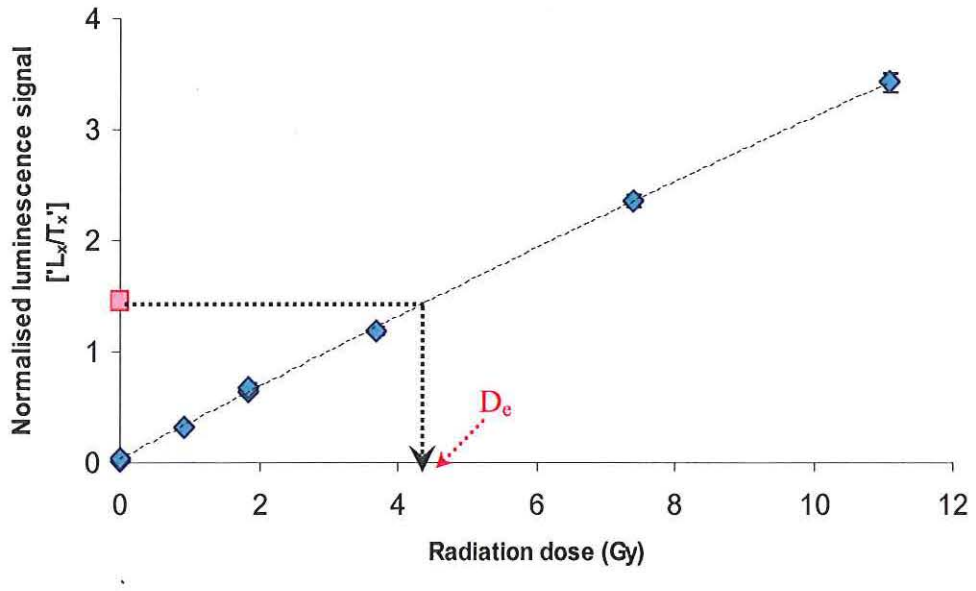

Figure 8: Typical growth curve constructed for aliquots in this OSL dating study. The example shown is from an aliquot of sample 73BH-1/1, which was preheated to 220°C/10s.

Once the sequence of dating measurements was completed, each aliquot was irradiated and then stimulated using infra-red (IR) laser-diodes at a temperature of 125°C to check the purity of each aliquot. Stimulation with IR was proposed as a check on the purity of prepared quartz material by Stokes (1992). Feldspathic minerals respond to simulation with IR, giving a rapidly decaying signal, however, quartz does not appear to respond to stimulation with IR (Spooner and Questiaux 1989). There was little evidence of any response above background signal levels to stimulation with IR for any aliquot in this study (a typical IR stimulated luminescence signal response is shown in Fig 9). No feldspar contamination was therefore considered to be present in any of the quartz separates prepared for this OSL dating study.

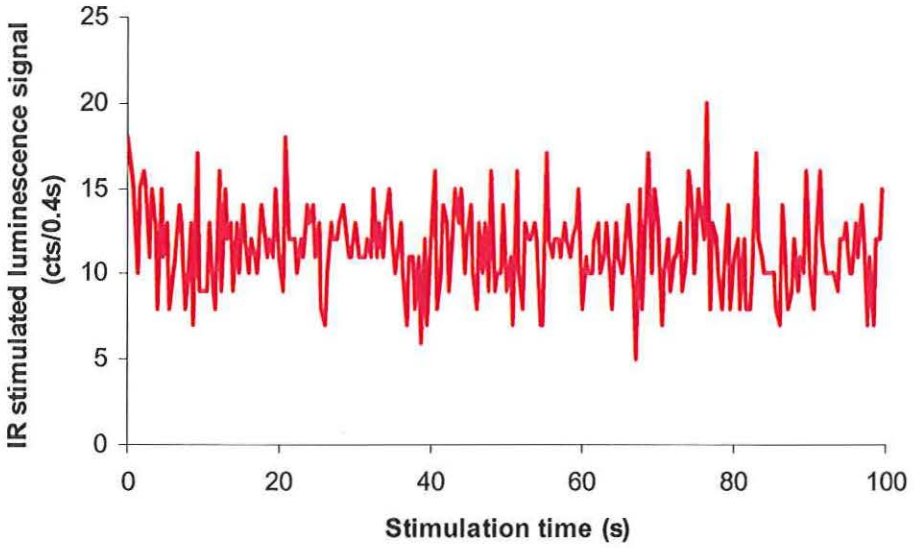

Figure 9: Typical response to stimulation with IR. The signal level is very low, being approximately at background levels, thereby suggesting that no feldspar is present in the quartz material prepared for OSL dating. The example shown is from an aliquot of sample 73BH-1/1 which was preheated to 220°C/10s.

7.4 Recovery of a known laboratory irradiation dose

An important test of any luminescence dating protocol employed is whether the value of a previously delivered laboratory irradiation dose can be accurately and precisely determined. This is sometimes referred to as a 'dose-recovery' test and should be conducted on material which has not previously received any thermal pre-treatments. This fundamental test was conducted for three aliquots of every sample in this dating study.

The laboratory beta dose chosen for the dose-recovery experiment was selected to be similar in magnitude to the D_e obtained for each sample. Three aliquots of each sample were prepared in the same way as the aliquots used for dating. The natural signal was removed from each aliquot by 1000s stimulation with blue diodes at room temperature, and a beta dose was then applied to each of the three aliquots. The SAR protocol was then applied using regeneration and test dose values of the same size as used in the dating measurement sequences, and applying a preheat of 220°C for 10s, and a cut heat of 160°C. The beta dose applied to each set of sample aliquots which was to be recovered is given in Table 5, both in grays (Gy) and also shown relative to the mean D_e of each sample after OSL dating. The beta dose recovered is also shown relative to the beta dose applied, based on the mean of three aliquots (Table 5). For each sample, the beta dose applied is recovered to within ± 10%, and more than 80% of the samples recover a dose to within ± 5%. The SAR measurement protocol therefore seems to be appropriate and working well for the sample material used for dating in this study.

7.5 OSL dating measurements and checks

The SAR measurement sequence employed in this study has several checks built into it to monitor the behaviour of the sample and the efficacy of the sensitivity correction. For each sample, a minimum of 21 aliquots was examined to establish D_e values for use in determining an OSL age, and up to 72 aliquots in the case of some samples where further tests were conducted in addition to the determination of D_e. The advantage of working with single-aliquot, rather than multiple-aliquot methods, is that each of the 21-72 aliquots measured gives rise to an independent assessment of D_e, and hence, potentially to an OSL age.

Working with a number of aliquots offers the advantage of making measurements using a range of thermal pre-treatments, to compare the D_e values determined for aliquots using different preheat temperatures. Thermal pre-treatments are employed in order to remove any unstable trapped charge prior to measurement of either the natural or an artificially irradiated OSL signal. However, high preheat temperatures are sometimes problematic for young samples, and can lead to erroneously high D_e values being determined due to thermal transfer of trapped charge from relatively stable yet optically-insensitive traps into OSL traps during preheating (eg Bailey *et al* 2001). Given the likely young age of the samples in this study, it was therefore of particular importance to make OSL measurements using a range of preheat temperatures to try to establish a preheat plateau where common values of D_e could be identified and any erroneously high D_e values could be discounted. A range of preheat temperatures was therefore investigated during OSL dating measurements of each sample, increasing to the given temperature at a rate of 5°C/s and held for 10s on reaching the required temperature; a minimum of three aliquots were examined at each of 7 preheat temperatures (160°C, 180°C, 200°C, 220°C, 240°C, 260°C, and 280°C) in cases where 21 aliquots were measured, and in the case of 24 aliquots an additional preheat temperature of 300°C was also used. Where more than 24 aliquots have been examined, these aliquots are distributed evenly across these eight preheat ranges.

An example of a preheat plot generated for samples in this study is shown in Figure 10, showing D_e values for each of three aliquots measured using one of eight preheat temperatures. For preheat temperatures between 160-260°C the D_e values determined are similar, giving a flat 'plateau' region on the graph. However, the value of D_e determined increases for aliquots measured using a preheat temperatures of 280°C or 300°C. This is believed to be due to thermal transfer of trapped charge, and hence these results were not used in the final calculation of the age of the sample.

Table 5: Recovery of a known beta dose for three aliquots prepared from each sample dated in this OSL study.

Sample	Dose applied (Gy)	Dose applied / Mean D_e	Dose recovered / Dose applied (mean of 3 aliquots)
73BH-1/1	1.85	0.5	0.95 ± 0.07
73BH-1/2	1.85	0.5	0.95 ± 0.03
73BH-1/3	1.85	0.4	0.97 ± 0.02
73BH-2/1	1.85	0.5	0.99 ± 0.02
73BH-2/2	1.85	0.5	1.01 ± 0.04
73BH-2/3	1.85	0.4	1.02 ± 0.03
73BH-3/1	1.85	0.8	0.96 ± 0.08
73BH-3/2	1.85	0.8	0.98 ± 0.01
73BH-3/3	1.85	0.5	1.00 ± 0.05
73BH-4/1	1.85	1.4	0.98 ± 0.01
73BH-4/2	1.48	0.8	0.96 ± 0.04
73BH-4/3	1.48	0.6	1.03 ± 0.08
73BH-5/1	1.11	0.8	1.04 ± 0.07
73BH-5/2	1.11	0.8	1.02 ± 0.07
73BH-6/1	1.39	1.3	0.99 ± 0.07
73BH-6/2	1.39	1.0	1.09 ± 0.01
73BH-6/3	1.39	0.9	1.01 ± 0.03
73BH-7/1	1.11	0.9	0.96 ± 0.06
73BH-7/2	1.11	0.9	1.01 ± 0.04
72BH-7/3	1.11	0.9	1.06 ± 0.08
73BH-8/1	0.46	0.6	0.97 ± 0.05
73BH-8/2	0.46	0.7	1.01 ± 0.04
73BH-8/3	0.46	0.5	1.03 ± 0.06
73BH-9/1	0.74	1.3	1.07 ± 0.08
73BH-9/2	1.11	1.1	1.05 ± 0.18
73BH-9/3	1.11	1.1	1.05 ± 0.03
73BH-10/1	0.55	1.0	0.96 ± 0.05
73BH-10/2	0.55	0.8	0.93 ± 0.13
73BH-10/3	1.29	1.0	0.98 ± 0.05
73BH-11/1	0.46	1.3	1.05 ± 0.12
73BH-11/2	0.46	1.0	0.98 ± 0.01
73BH-11/3	0.46	0.6	1.10 ± 0.12
73BH-12/1	0.46	0.9	1.04 ± 0.01
73BH-12/2	0.46	1.0	1.05 ± 0.06
73BH-12/3	0.46	1.0	1.08 ± 0.08
73BH-13/1	1.11	1.5	0.93 ± 0.14
73BH-13/2	1.11	1.3	0.99 ± 0.07
73BH-13/3	1.11	1.0	1.01 ± 0.05
80MP-1	0.28	0.9	1.04 ± 0.27

a)

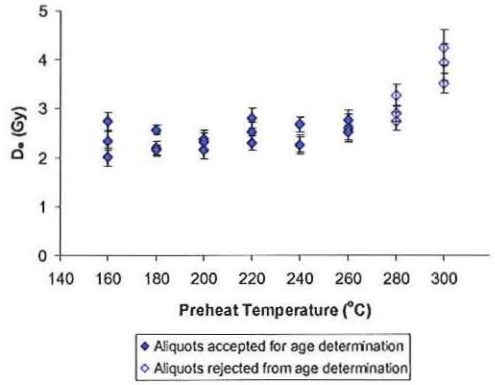

b)

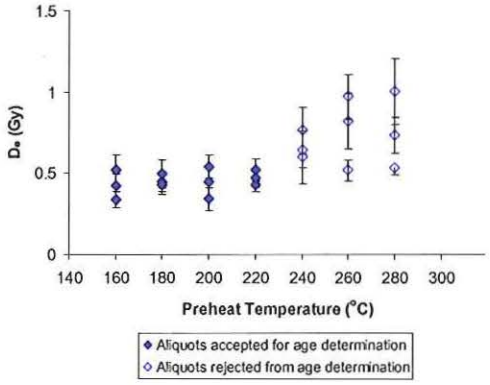

Figure 10: Examples of preheat plots used in this study, showing the D_e value determined for each of the three aliquots measured using a range of different preheat temperatures. The associated error in D_e is from the error on 'n' as defined by Galbraith (2002) from counting statistics and the error associated with curve fitting as used in *Analyst* (written by Dr. Geoff Duller, University of Wales, Aberystwyth). Fig a) shows an example where a total of 24 aliquots are examined, taken from sample 73BH-3/2, b) shows an example where 21 aliquots are examined and the preheat plateau spans a narrower range, sample 73BH-11/2.

Fifteen of the samples in this study, selected at random, were measured using a preheat temperature of 300°C; in all cases, this preheat temperature was found to be unsuitable for the samples, giving rise to erroneously high values of D_e (as shown in Fig 10a, and discussed above). This preheat temperature was therefore abandoned for the remainder of the study.

A preheat temperature of 280°C also proved to be too aggressive for most samples studied (with the exception of sample 73BH-5/2), however its measurement is still valuable because it is acceptable in some cases and it can help to identify the plateau region of a preheat plot (eg Fig 10a). The value of measuring aliquots using a range of preheat temperatures is demonstrated by the fact that the preheat plateau region spanned between 160-280°C for some samples, yet only between around 160-220°C for others (eg Fig 10b).

Aside from the plateau test, which examines the effect of different preheat temperatures, other criteria may be used to evaluate the behaviour and reliability of the aliquots used for dating. One of the most powerful of these tests arises from the use of the SAR protocol for the OSL dating measurements. In this measurement procedure, the natural luminescence signal is measured, followed by the response to a series of artificial laboratory beta doses of increasing magnitude designed to bracket the intensity of the natural signal (Table 2). In the SAR measurements made in this study, a low irradiation dose was then repeated, or recycled, and applied at the end of the measurement cycle for all aliquots to test how well the sensitivity correction

procedure is working. If the sensitivity correction is adequate, then the ratio of the signal arising from this repeated regenerative dose at the end of the measurement sequence to that of its earlier regeneration dose (eg Table 2) should fall within the range of 1 ± 0.1 (Murray and Wintle 2000). Only 11 of the 1102 aliquots examined for OSL dating failed this 'recycling test' (detailed in Table 6), indicating that the sensitivity correction in the SAR measurement procedure is working well for these samples in monitoring and correcting for changes in luminescence sensitivity that may have occurred as a function of time, temperature, and past-radiation exposure.

A further test of the reliability of the sensitivity corrected growth curve generated using the SAR measurement protocol is a check on the 'recuperation' of signal (Murray and Wintle 2000) following the application of a regeneration dose of 0 Gy at both the beginning (following measurement of the natural signal) and towards the end of the measurement cycle (following the largest regeneration dose and prior to the application of the recycling regeneration dose). No significant net OSL signal should be observed following this 0 Gy beta dose if the sensitivity correction is working correctly. At lower preheat temperatures, no recuperation in OSL signal was observed and the dose-response or 'growth' curve generated passed through the origin (eg Fig 11a). However, at higher preheat temperatures, the samples in the study showed an increasing level of signal recuperation (eg Fig 11b); again, this is an indication that thermal transfer of charge is occurring from optically insensitive traps into OSL traps at higher preheat temperatures. Those aliquots identified from their preheat plot as having erroneously high D_e values at high temperatures (Table 6), also showed significant recuperation of signal.

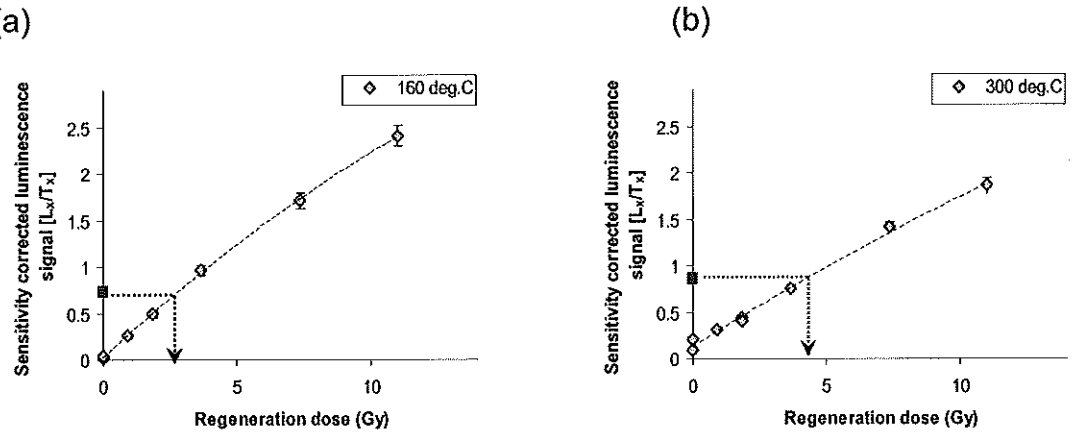

Figure 11: Sensitivity corrected dose-response or 'growth' curves measured following (a) low (160°C) and (b) high (300°C) preheat temperatures for the aliquots shown in the preheat plot of Figure 10 (sample 73BH-3/2). Note that for (b), the sensitivity corrected value for the natural OSL signal (denoted by the square symbol plotted on the y-axis) and the D_e value obtained (Gy) are both higher than for the low preheat temperature aliquot. In addition, the dose-response curve does not pass through the origin, and an increase in recuperation of the OSL signal is also observed between the beginning and the end of the measurement sequence. In spite of this, the aliquot still passes

the recycling ratio test (repeating a regeneration dose at the end of the measurement sequence, here of ~2 Gy).

7.6 Determination of the equivalent dose for use in the final OSL age calculation

The aliquots on which OSL dating measurements were conducted were screened for their suitability for use in the final age equation using the series of tests described and discussed above. These checks included examination of signal intensity levels, decay curve shape, growth curve shape, recycling ratio, recuperation, preheat plots, and feldspar contamination checks using IR stimulation. Table 6 lists the number of aliquots rejected from the suite of OSL dating measurements for each sample, giving reasons for rejection. The most common reason for rejection of aliquots (accounting for 88% of the aliquots rejected) was on the basis of high D_e determinations at preheat temperatures that proved to be too high for that particular sample. Of the total of 1102 OSL dating aliquots examined in this study, 32% were rejected following various checks during analysis of the data. In spite of this, the minimum number of acceptable aliquots combined to determine a final OSL age for any sample was at least 12. In some cases, where measurements had also been made using various aliquot sizes, up to 44 aliquots were used in the final OSL age calculation.

For each sample, the D_e values of the aliquots accepted following screening were normally distributed (an example is shown in Fig 12). The simple arithmetic mean of these D_e values was therefore taken for calculation of the final OSL age (discussed in section 8). The error on each determination of D_e was calculated using the standard error (ie the standard deviation divided by the square root of the number of estimates of D_e). The D_e and standard error are given for each sample in the final OSL age tables (Tables 7.1 - 7.15).

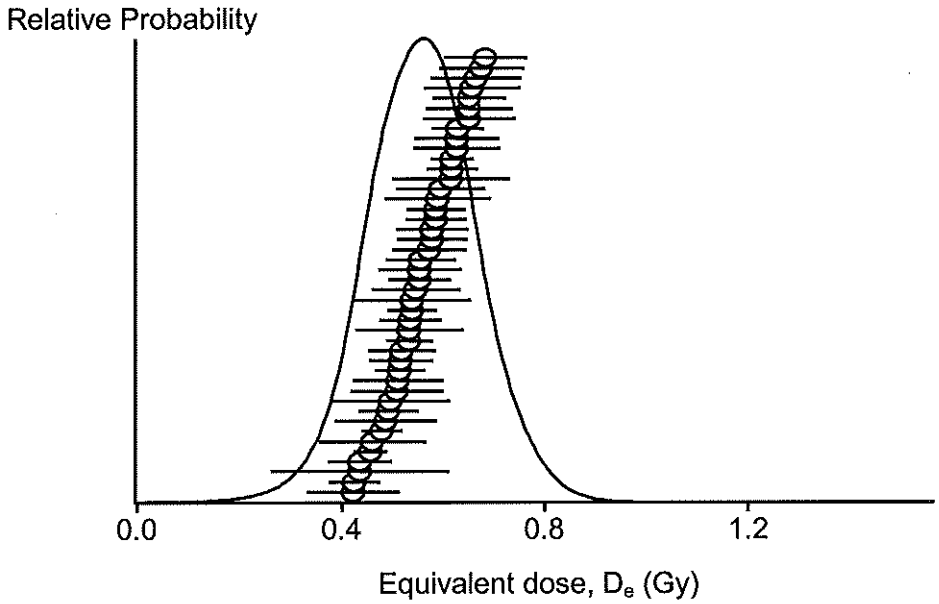

Figure 12: The distribution of D_e values obtained for a sample where a large number of aliquots were measured, namely sample 73BH-10/1. The 44 aliquots shown here in this probability density plot, clearly demonstrate that this sample is normally distributed, as are all of the samples in this OSL dating study.

Table 6: Number of aliquots rejected from each suite of OSL dating measurements for each sample dated, and the reasons for rejection.

Core number	Sample 1	Sample 2	Sample 3
73 BH 1	6 @ 300°C, 6 @ 280°C, 5 - notably high D_e values (31/48 accepted)	6 @ 300°C, 6 @ 280°C, 1 - notably high D_e value, 2 – failed recycling test (33/48 accepted)	3 @ 300°C, 3 - notably high D_e values (18/24 accepted)
73 BH 2	3 @ 300°C, 3 @ 280°C (18/24 accepted)	3 @ 300°C, 3 @ 280°C, 1 – failed recycling test (17/24 accepted)	3 @ 300°C, 3 @ 280°C, 3 @ 260°C, 3 @ 240°C (12/24 accepted)
73 BH 3	3 @ 300°C, 3 @ 280°C, 1 – notably high D_e value (17/24 accepted)	3 @ 300°C, 3 @ 280°C (18/24 accepted)	3 @ 300°C, 3 @ 280°C, 1 - notably high D_e value (17/24 accepted)
73 BH 4	3 @ 280°C, 1 - notably low D_e value (17/21 accepted)	3 @ 280°C (18/21 accepted)	3 @ 280°C, 3 @ 260°C, 2 - notably high D_e values, (13/21 accepted)
73 BH 5	2 – failed recycling test (19/21 accepted)	3 @ 280°C (18/21 accepted)	n/a
73 BH 6	3 @ 300°C, 3 @ 280°C, 3 @ 260°C, 1 – failed recycling test (14/24 accepted)	3 @ 300°C, 3 @ 280°C, 3 @ 260°C (15/24 accepted)	6 @ 300°C, 6 @ 280°C, 6 @ 260°C, 4 @ 160°C (26/48 accepted)
73 BH 7	3 @ 280°C, 3 @ 260°C, 3 @ 240°C (12/21 accepted)	3 @ 280°C, 3 @ 260°C, 1 - notably high D_e value (14/21 accepted)	6 @ 280°C, 3 @ 260°C, 3 @ 160°C, 1 - notably high D_e value (29/42 accepted)
73 BH 8	3 @ 280°C, 3 @ 260°C (15/21 accepted)	3 @ 280°C, 3 @ 260°C, 1 - notably low D_e value, 1 – failed recycling test (13/21 accepted)	3 @ 280°C, 3 @ 260°C, 1 – failed recycling test (14/21 accepted)
73 BH 9	3 @ 280°C, 3 @ 260°C (15/21 accepted)	3 @ 280°C, 1 - notably high D_e value (17/21 accepted)	3 @ 280°C, 3 @ 260°C, 1 - notably high D_e value (14/21 accepted)
73 BH 10	9 @ 300°C, 9 @ 280°C, 9 @ 260°C, 1 - notably high D_e value (44/72 accepted)	6 @ 300°C, 6 @ 280°C, 6 @ 260°C, 3 - notably high D_e value (27/48 accepted)	3 @ 300°C, 3 @ 280°C, 3 @ 260°C, 1 - notably high D_e value (20/29 accepted)
73 BH 11	6 @ 280°C, 1 - notably high D_e value (35/42 accepted)	3 @ 280°C, 3 @ 260°C, 3 @ 240°C (12/21 accepted)	3 @ 280°C, 3 @ 260°C, 1 - notably high D_e value (14/21 accepted)
73 BH 12	6 @ 280°C, 3 @ 260°C, 1 - notably high D_e value (32/42 accepted)	3 @ 280°C, 3 @ 260°C, 1 - notably high D_e value (14/21 accepted)	3 @ 280°C, 3 @ 260°C (15/21 accepted)
73 BH 13	6 @ 280°C, 6 @ 260°C, 3 @ 240°C, 1 - notably high D_e value, 2 – failed recycling test (24/42 accepted)	3 @ 280°C, 3 @ 260°C, 1 – failed recycling test (14/21 accepted)	3 @ 280°C, 3 @ 260°C (15/21 accepted)
80 MP 1	3 @ 280°C, 3 @ 260°C, 1 - notably high D_e value (19/26 accepted)	n/a	n/a

The aliquots which were accepted following all the screening tests are shown for each sample in Figures 13.1 – 13.15, for all OSL dating samples examined plus the two modern analogue surface samples. The distribution of D_e values are presented as radial plots (Galbraith 1990), with the D_e of each aliquot being shown as a single point on the plot. These plots are presented as a visual aid to the data only, and displaying the data on such plots offers the advantage of showing the precision to which each data point is known. The precision is displayed on the x-axis, with data of high precision being plotted towards the right hand side of the plot. The y-axis shows the number of standard deviations away from a central value for each D_e value, whilst the radial scale displays the D_e value. The horizontal dotted line extending from 0 on the y-axis is the mean D_e calculated for the sample. The dotted lines extending from the y-axis to the radial scale in s 13.1 - 13.15 are placed at two standard deviations, and any points falling within these limits (indicated by infilled circles) therefore lie within two standard deviations of the mean D_e value. Ideally, the data for all aliquots will fall within this band indicated on the diagrams, indicating one population of D_e values. The data for each sample in this study show very little scatter in the distribution of D_e values obtained following screening (Figs 13.1 - 13.15), suggesting only one population of D_e values for each sample.

Figure 13.1: Distribution of equivalent dose (D_e) values used for the determination of OSL ages for deep drill core 1, Broomhill Farm.

73BH 1/1

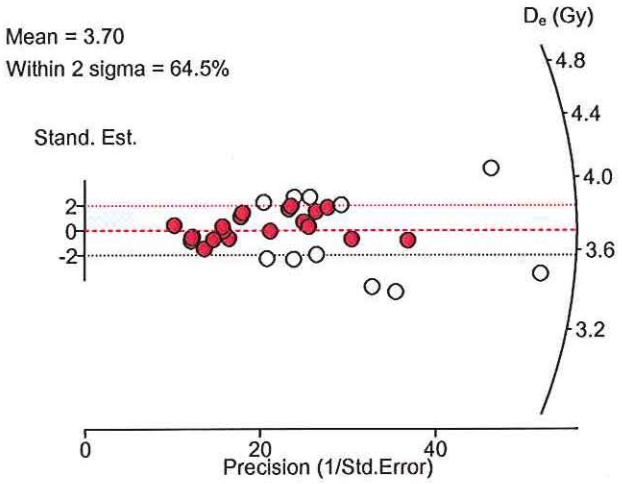

73BH 1/2

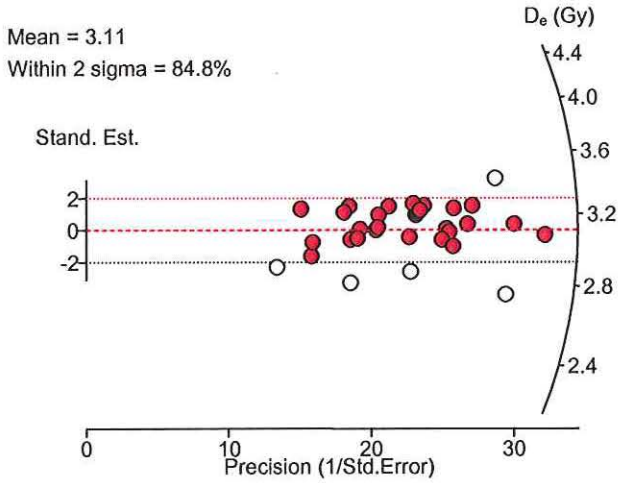

73BH 1/3

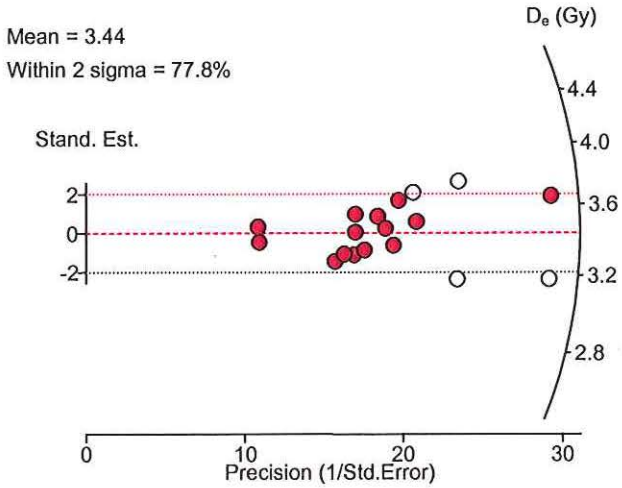

Figure 13.2: Distribution of equivalent dose (D_e) values used for the determination of OSL ages for deep drill core 2, The Midrips.

73BH 2/1

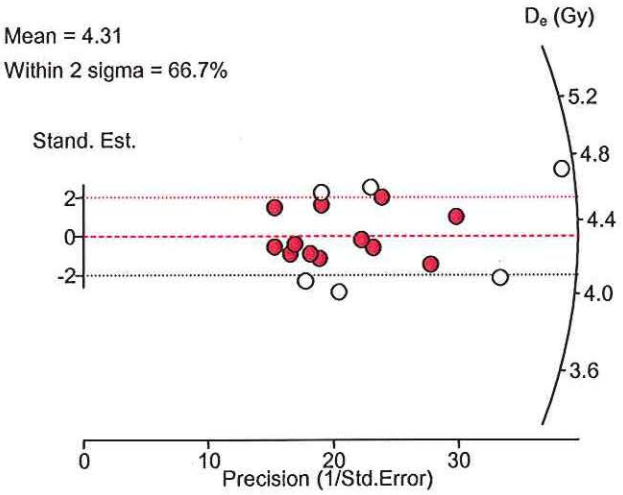

73BH 2/2

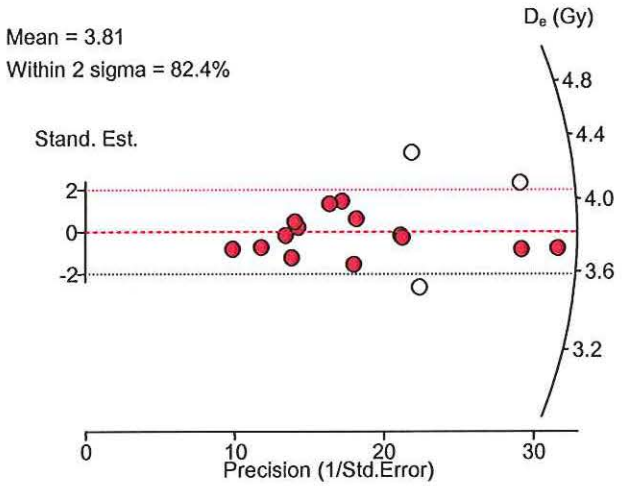

73BH 2/3

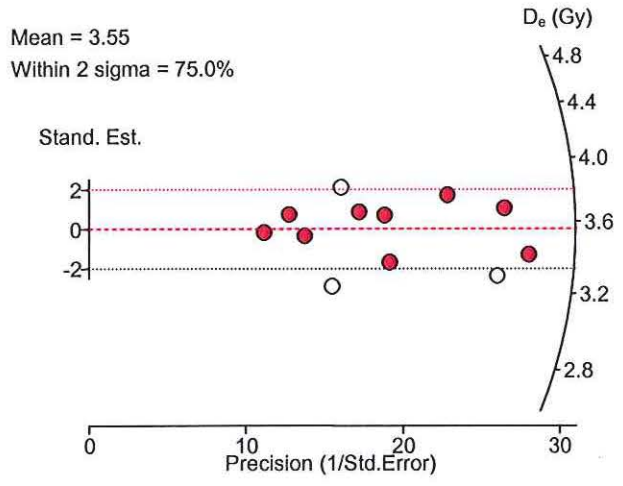

Figure 13.3: Distribution of equivalent dose (D_e) values used for the determination of OSL ages for deep drill core 3, The Forelands.

73BH 3/1

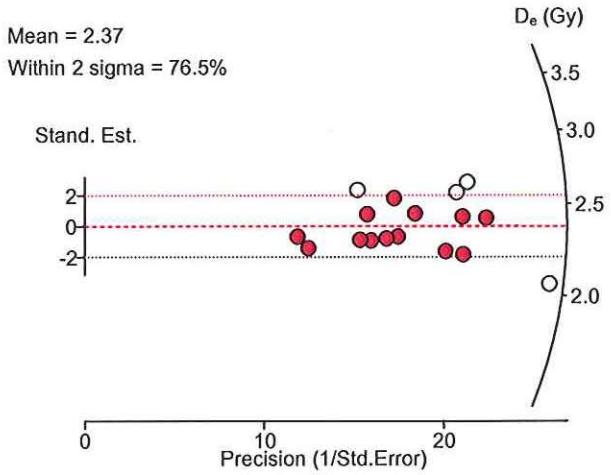

73BH 3/2

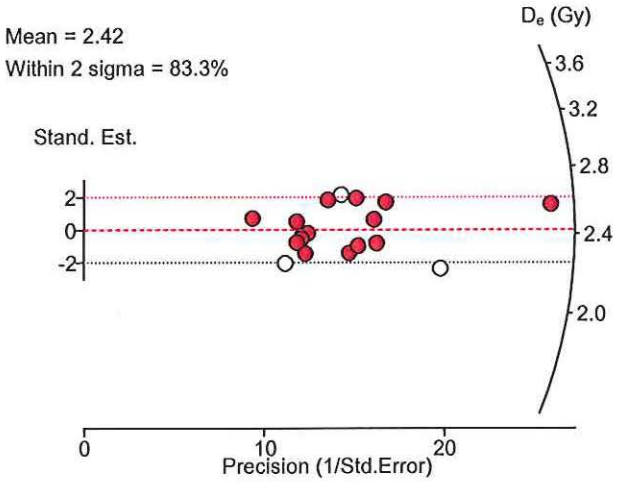

73BH 3/3

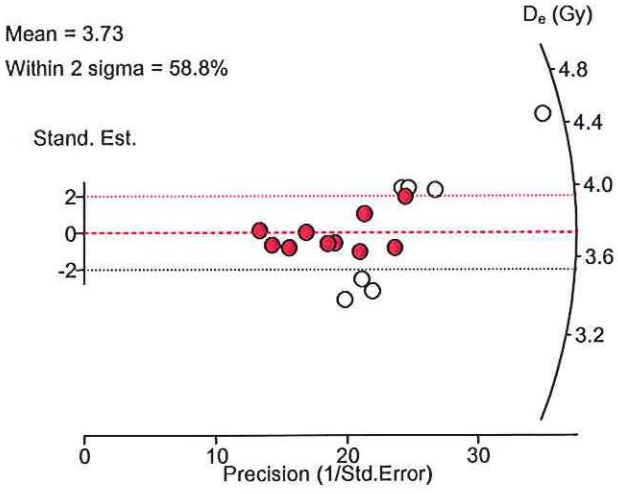

Figure 13.4: Distribution of equivalent dose (D_e) values used for the determination of OSL ages for deep drill core 4, Holmstone.

73BH 4/1

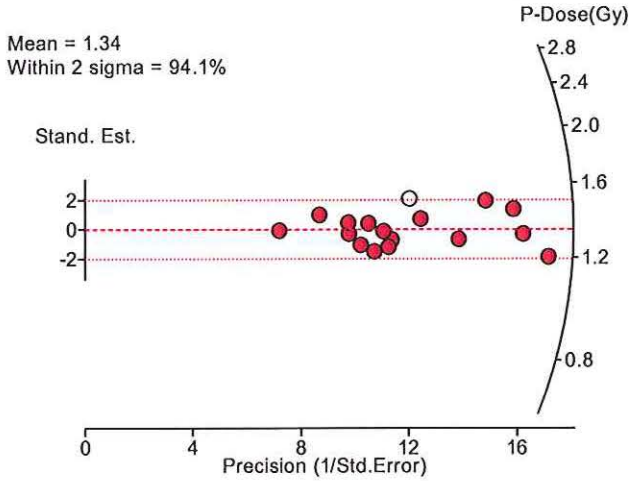

73BH 4/2

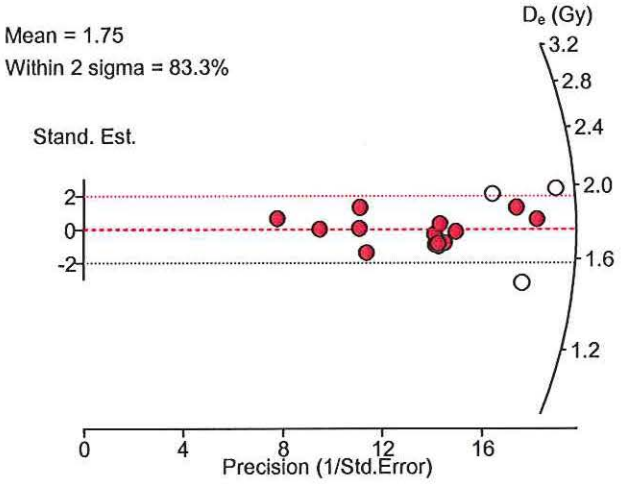

73BH 4/3

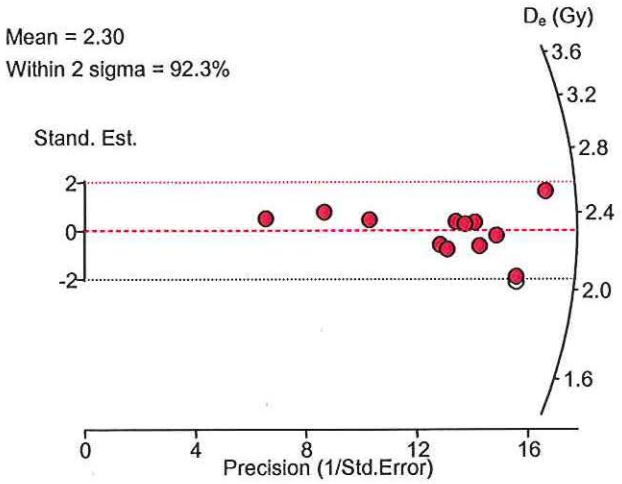

Figure 13.5: Distribution of equivalent dose (D_e) values used for the determination of OSL ages for deep drill core 5, South Brooks.

73BH 5/1

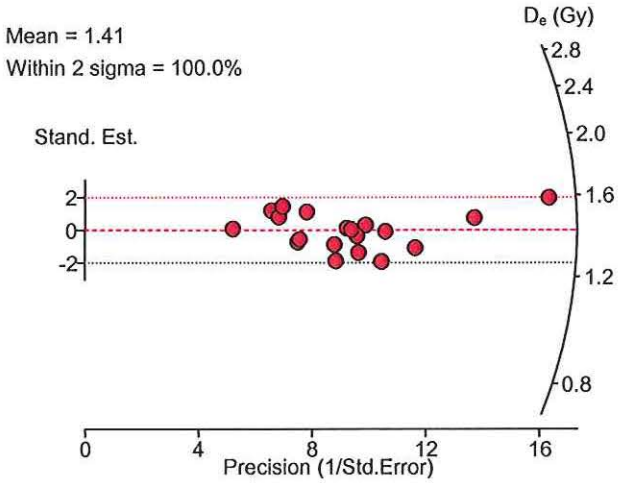

73BH 5/2

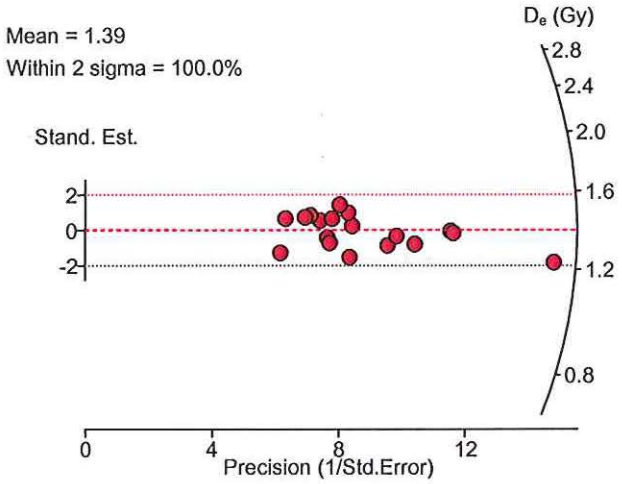

Figure 13.6: Distribution of equivalent dose (D_e) values used for the determination of OSL ages for deep drill core 6, Dungeness Road Gate.

73BH 6/1

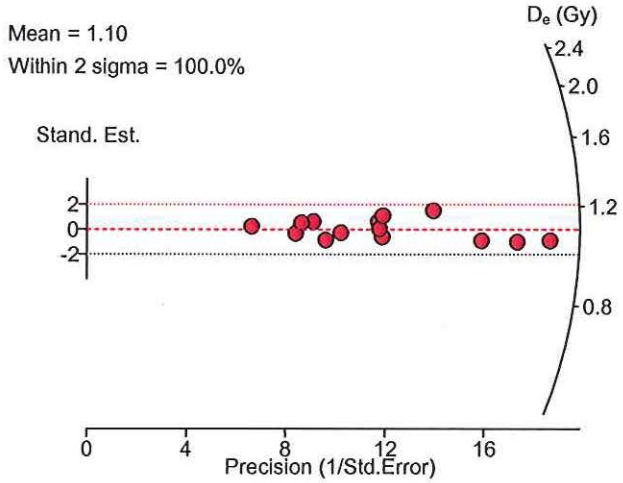

73BH 6/2

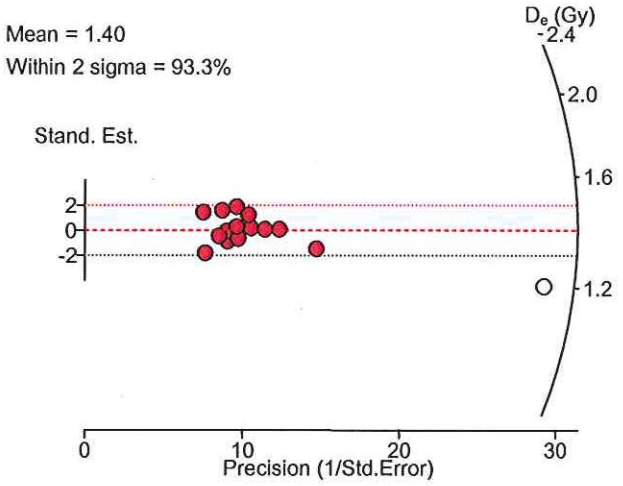

73BH 6/3

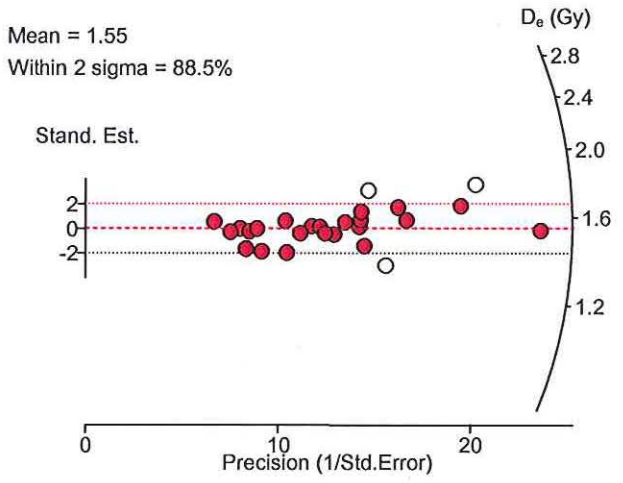

Figure 13.7: Distribution of equivalent dose (D_e) values used for the determination of OSL ages for deep drill core 7, Dengemarsh Road.

73BH 7/1

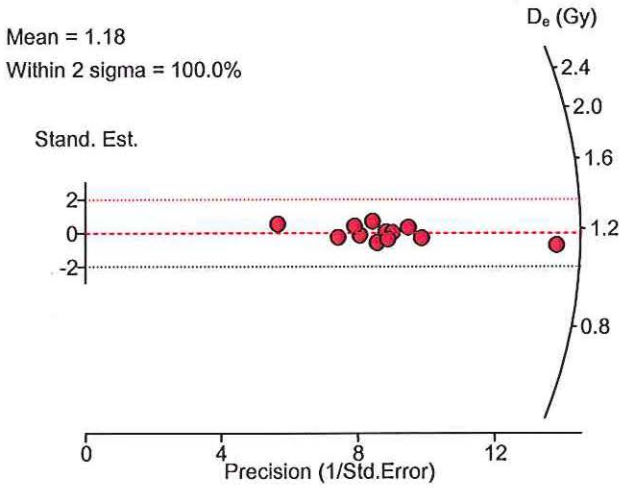

73BH 7/2

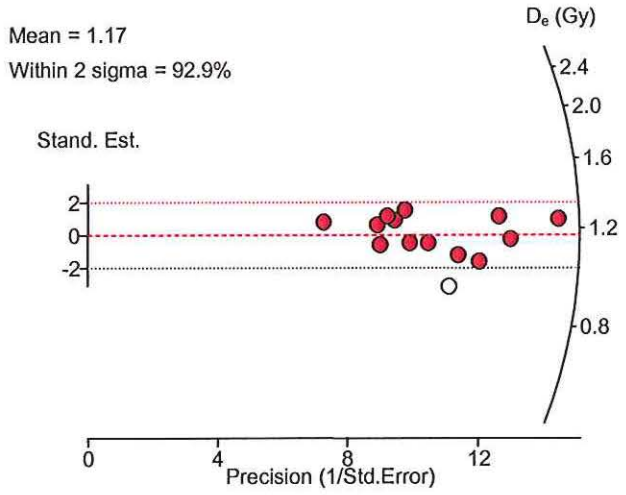

73BH 7/3

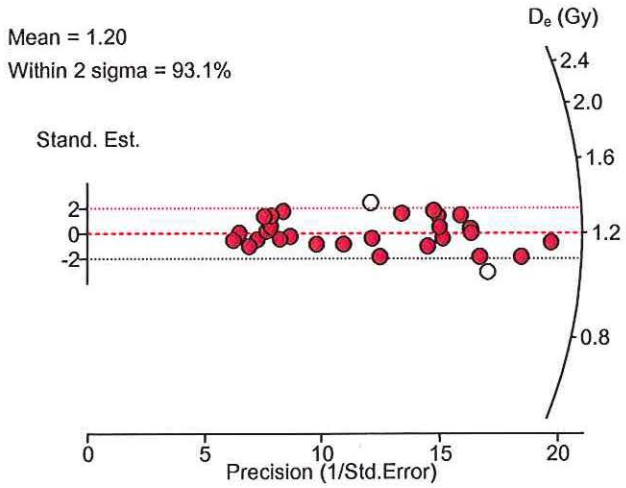

Figure 13.8: Distribution of equivalent dose (D_e) values used for the determination of OSL ages for deep drill core 8, Dungeness Lookout.

73BH 8/1

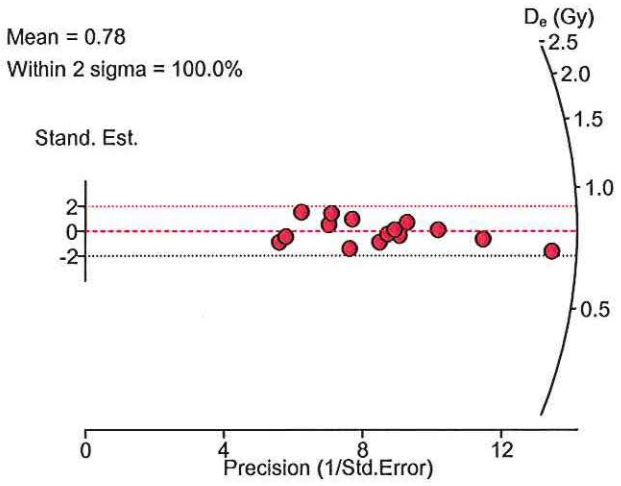

73BH 8/2

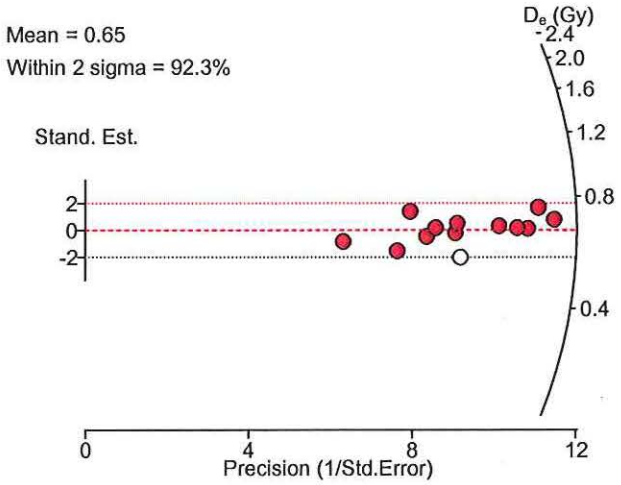

73BH 8/3

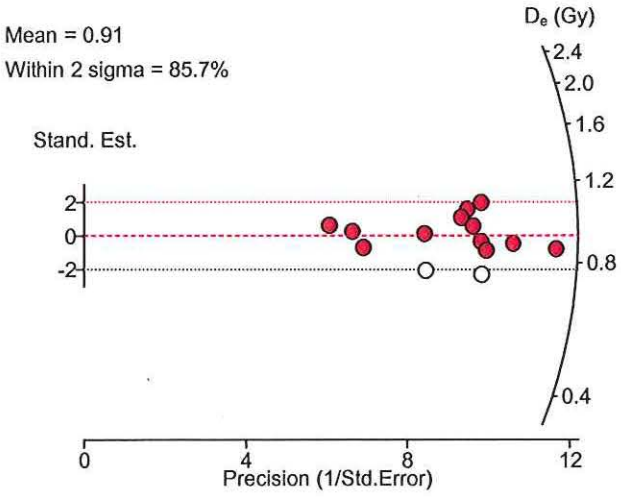

Figure 13.9: Distribution of equivalent dose (D_e) values used for the determination of OSL ages for deep drill core 9, RSPB Visitor Centre.

73BH 9/1

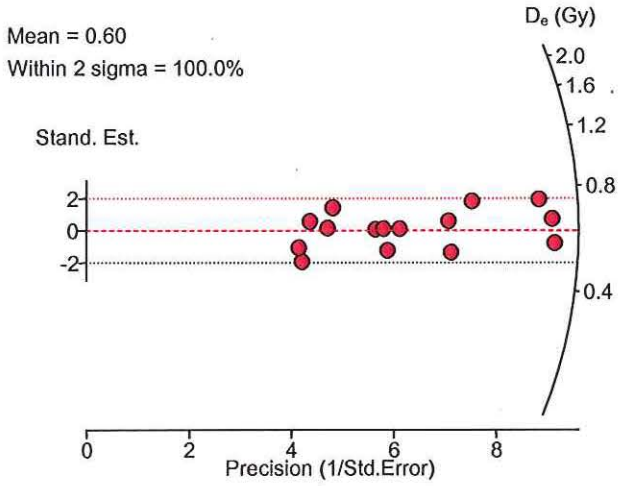

73BH 9/2

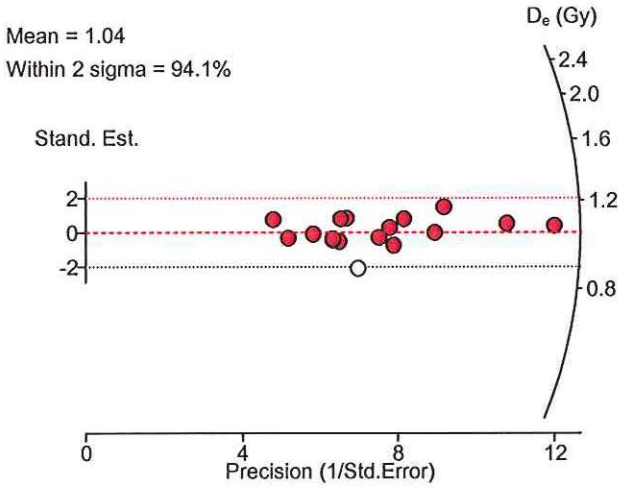

73BH 9/3

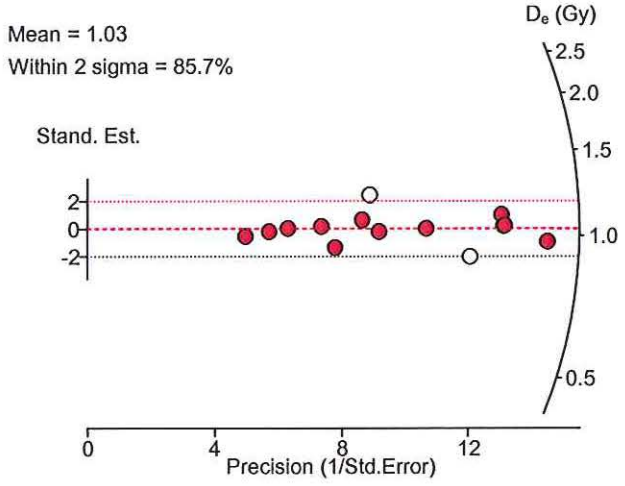

Figure 13.10: Distribution of equivalent dose (D_e) values used for the determination of OSL ages for deep drill core 10, ARC.

73BH 10/1

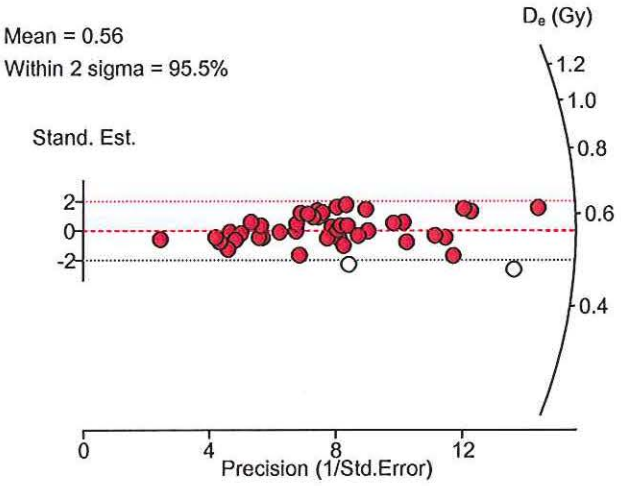

73BH 10/2

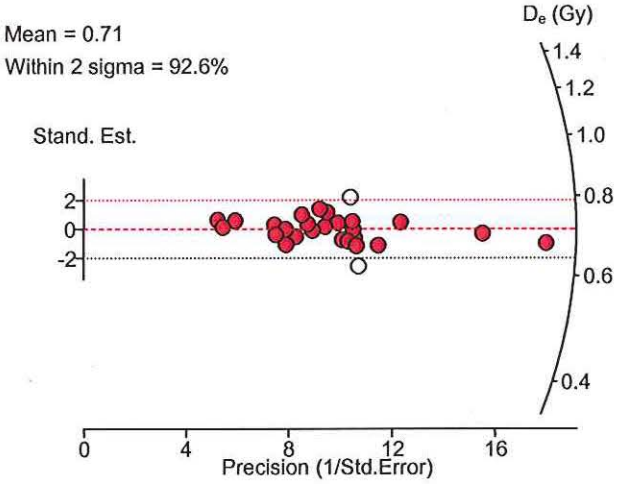

73BH 10/3

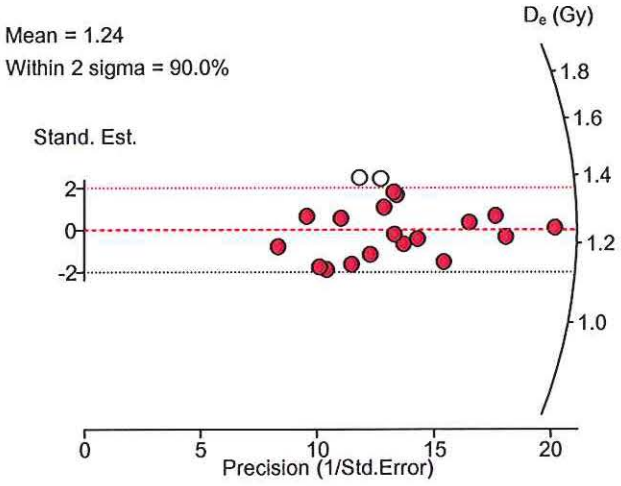

Figure 13.11: Distribution of equivalent dose (D_e) values used for the determination of OSL ages for deep drill core 11, Greatstone.

73BH 11/1

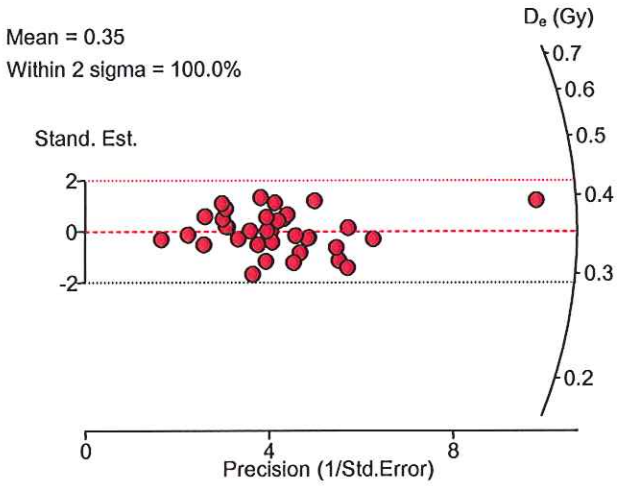

73BH 11/2

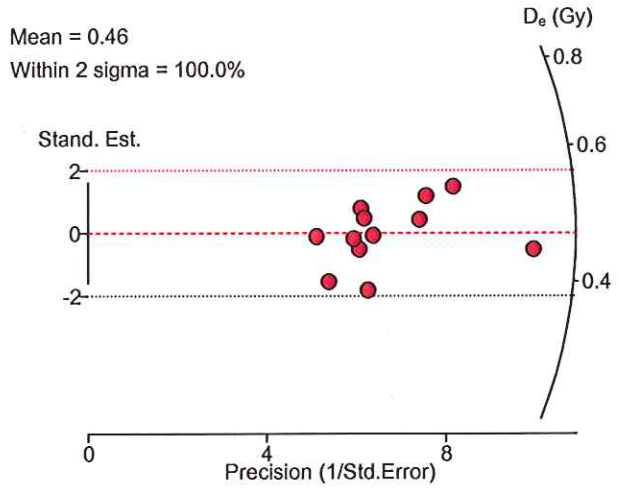

73BH 11/3

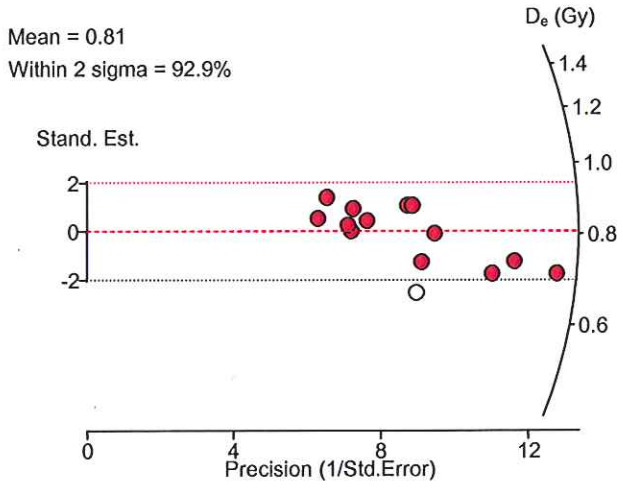

Figure 13.12: Distribution of equivalent dose (D_e) values used for the determination of OSL ages for deep drill core 12, Power Station.

73BH 12/1

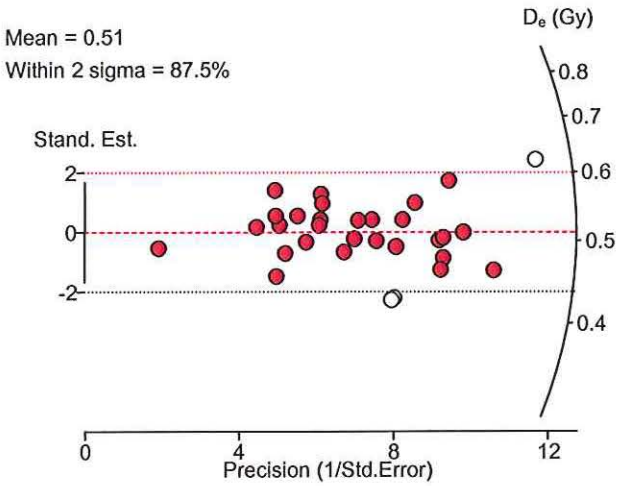

73BH 12/2

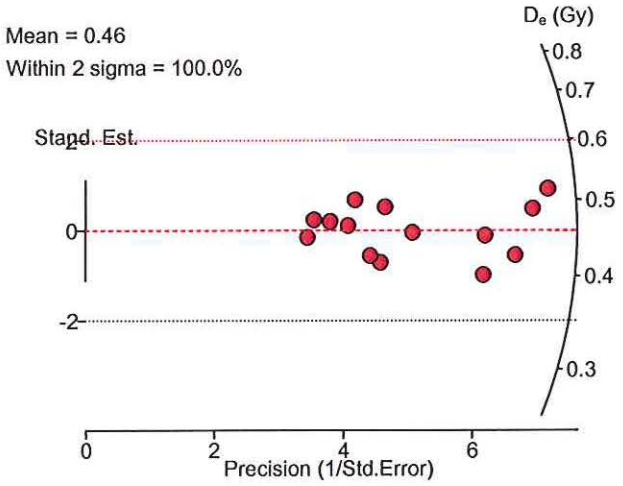

73BH 12/3

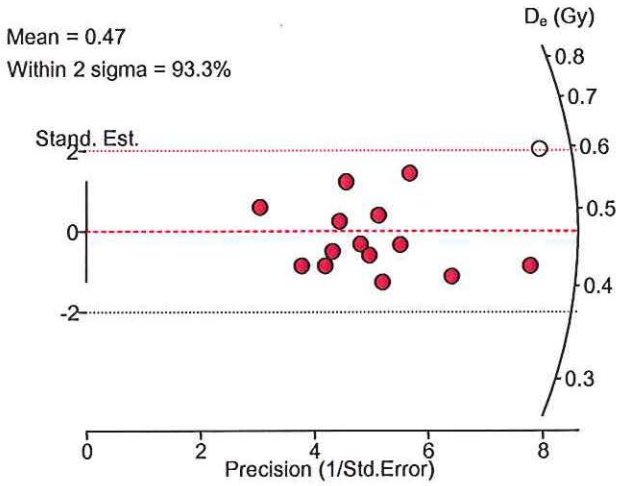

Figure 13.13: Distribution of equivalent dose (D_e) values used for the determination of OSL ages for deep drill core 13, Castle Farm.

73BH 13/1

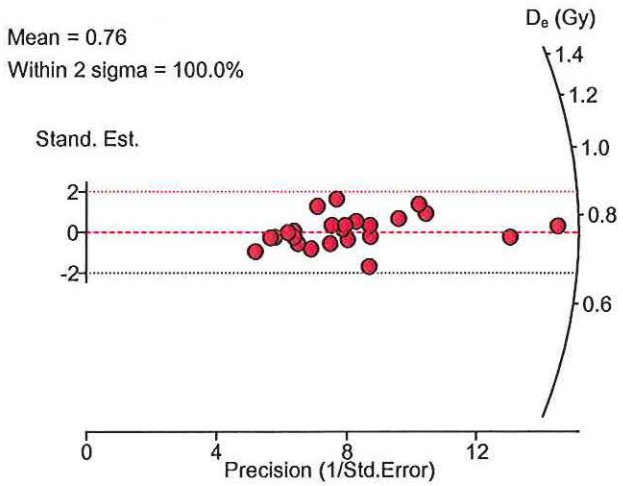

73BH 13/2

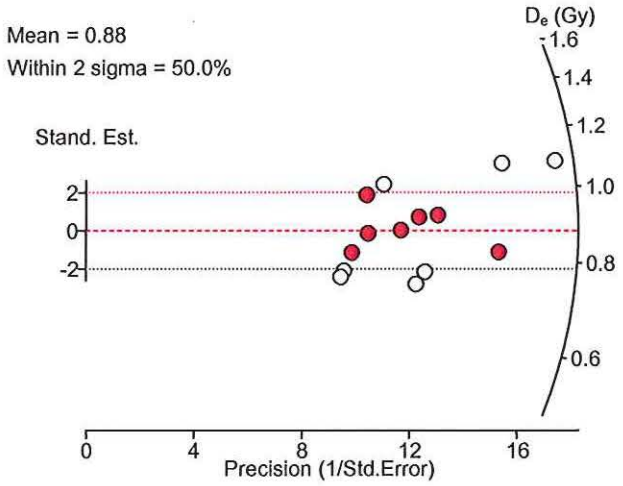

73BH 13/3

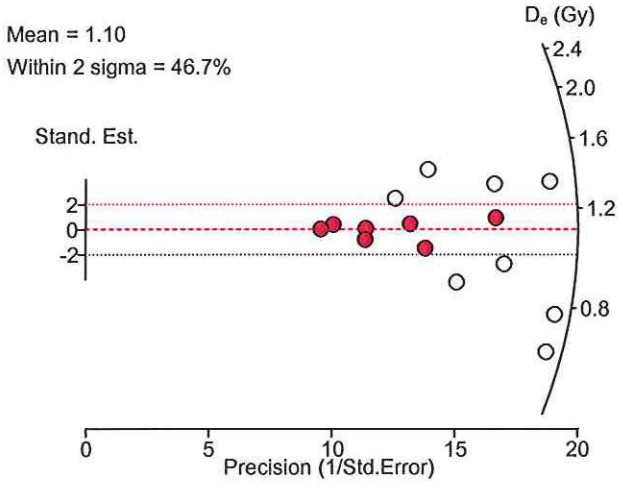

Figure 13.14: Distribution of equivalent dose (D_e) values used for the determination of OSL ages for shallow hand-core, Moneypenny Farm.

80MP 1

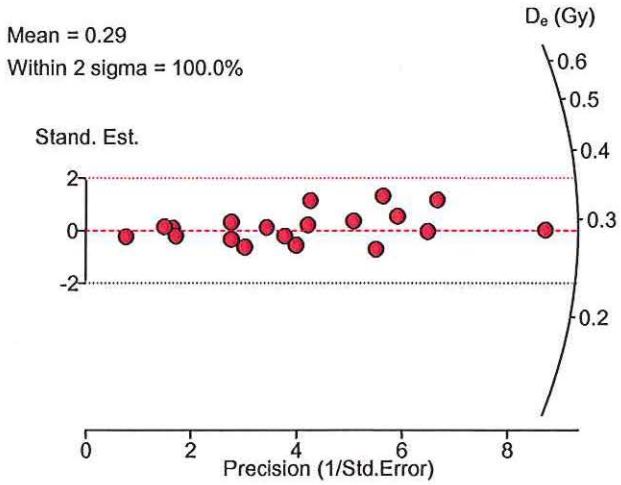

Figure 13.15: Distribution of equivalent dose (D_e) values used for the determination of OSL ages for modern analogue surface samples, Greatstone Beach.

73BH USS (Upper Shoreface Sands)

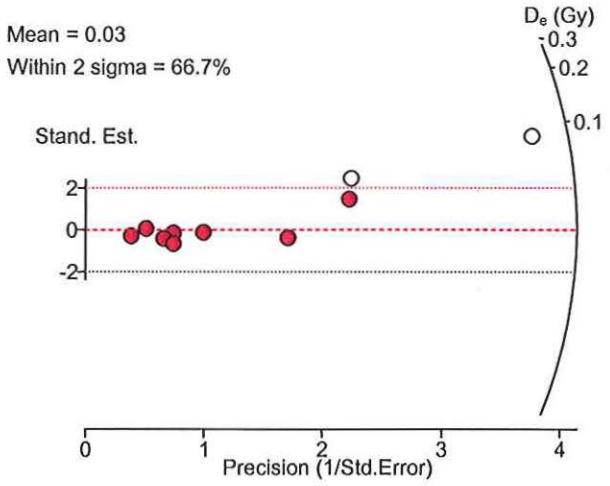

73BH SSR (Symmetrical Sand Ripples)

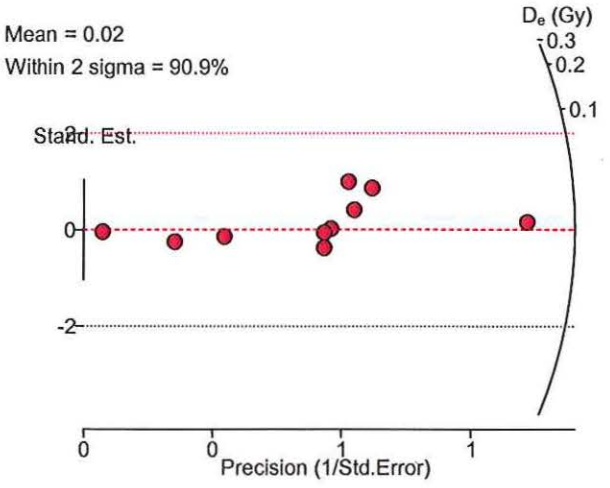

8. OSL age determinations

The equivalent dose (D_e) data and the results of laboratory dosimetry measurements were combined for each sample, with corrections being made for attenuation by water and for grain size, to give an OSL age for each of the 39 samples in this study, plus two modern analogue surface samples. These data, including the final age determinations, are presented in detail for each sample in Tables 7.1 – 7.15. The dose rate derived from U, Th and K is so low that the cosmic dose rate makes a significant contribution to the total dose rate. The error shown for the D_e determination of each of the 39 dating samples (Tables 7.1 – 7.14) is the standard error (see section 7.6) (ie the standard deviation divided by the square root of the number of independent estimates of D_e). The average percentage error on the OSL ages is 5.0 ± 0.8 %. These percentage errors increase as the age of the samples decreases; if cores with OSL ages older than ~1000 years are considered (ie cores 73BH-1 to -8), the average percentage error on the OSL ages is 4.7 ± 0.4 %.

The OSL age data for two modern analogue surface samples taken from Greatstone Beach in addition to the 39 core samples for dating, are given in Table 7.15. These modern samples were taken as a test of how well the samples in this study were likely to be bleached on deposition; if these surface samples give an OSL age of zero years, within errors, then they are considered to be well bleached on deposition. The samples were taken from the upper ~1cm of the beach from the upper shoreface sands (73BH-USS) and from symmetrical sand ripples (73BH-SSR) exposed at low tide. This environment is believed to be analogous to the environment of deposition of the sub-gravel sand samples dated in this study. The OSL data gave results equivalent to burial for 40 ± 40 years for the upper shoreface sands, and 15 ± 15 years for the symmetrical sand ripples (Table 7.15), suggesting that incomplete bleaching is not a problem for samples in this OSL dating study. Additionally, the consistency and reproducibility of replicate measurements made for other samples in this study suggest that the samples are well bleached.

For each of the 13 deep-drill cores and the short hand-core from Moneypenny Farm, the uppermost OSL sample was taken as close as possible to the stratigraphic change between the uppermost sandy gravel unit and the silty sand unit being dated using OSL, whilst maintaining a distance of at least 30cm between the sample and any change in stratigraphy to ensure a homogeneous dose rate to the sample. The lowest OSL sample was taken from towards the base of each drill core, but this was simply the deepest drill depth reached, rather than necessarily representing the end of the silty sand unit. Thus, comparison of the uppermost samples representing the top of the stratigraphic unit being dated offers the fairest spatial comparison of the OSL ages obtained in this study. The mean age (no errors shown) for the uppermost OSL sample in each of the sub-gravel sand cores in this study is shown in Figure 14. Looking at the Dungeness foreland (cores 1-12), the OSL ages relate well to each other, demonstrating a younging trend eastwards from Broomhill (core 1) towards the tip of the foreland at Dungeness Power Station (core 12). The uppermost OSL ages of the north-south transect cores

taken (cores 8-11) also show a trend of younging northwards. Collectively, the uppermost sub-gravel sand OSL ages (Fig 14) suggest that the sub-gravel sands were deposited not as a simple eastwardly development of the shoreline but rather, perhaps, as a spit-like formation, with younger sediments being deposited both to the north and the east of the foreland. The OSL ages show that the uppermost sub-gravel sands were deposited between ~4700 and ~400 years ago. These OSL ages act as maximum limiting ages for the gravel which lies on top of the dated sand body, thereby constraining the time of deposition of the gravel. Likewise, the uppermost OSL ages for Camber Farm (Fig 14, core 13, sampled as part of the Rye project) and Moneypenny Farm ('MP' on Fig 14) also provide maximum limiting ages for the emplacement of the gravel overlying the dated sand unit, being ~600 and 500 years ago, respectively.

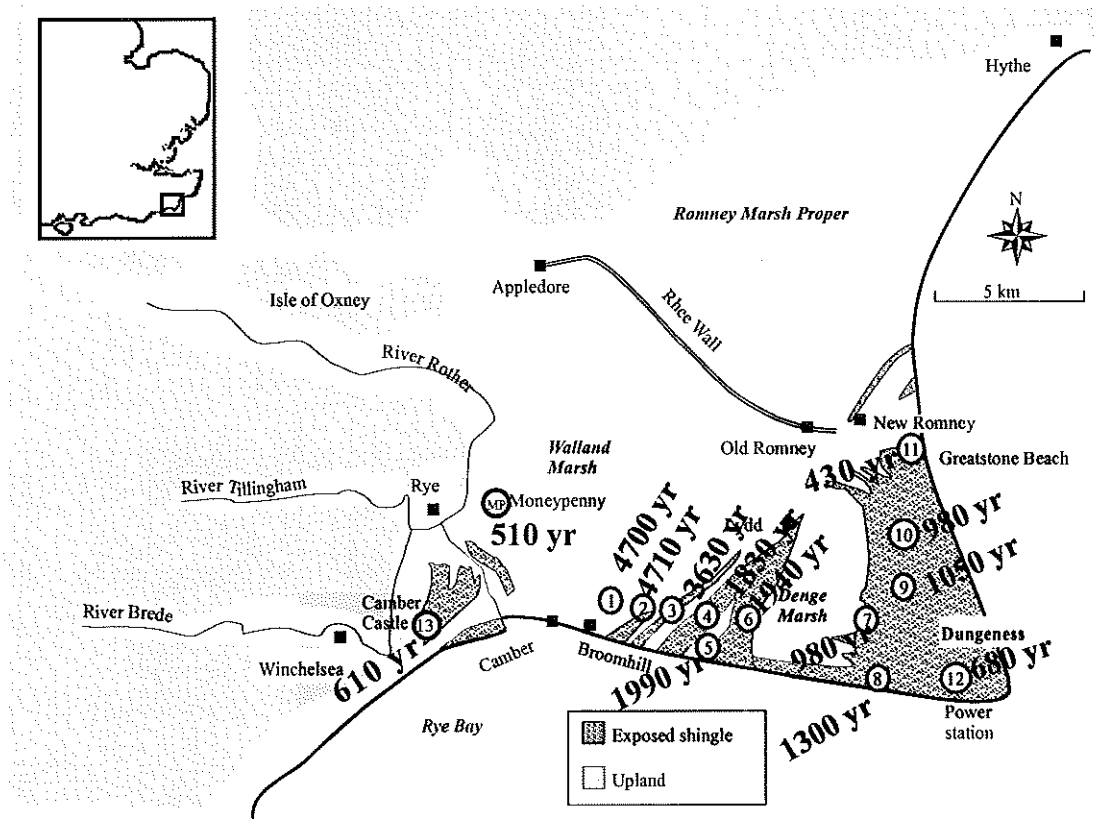

Figure 14: The uppermost OSL ages of the silty-sand unit dated for each core sample. The central OSL age is quoted with no error term, for simple comparison (see Tables 7.1 - 7.14 for details of the error on OSL ages).

The OSL ages of each sample taken from the sub-gravel sand unit of Dungeness Foreland (deep drill cores 1-12) are summarised in Figure 15 (OSL ages are shown with the standard error), showing the stratigraphic relationship between all 35 samples dated for (a) the west to east transect, and (b) the north to south transect. The deep drill core taken at Camber Farm as part of the Rye project is also shown in Figure 15b, to show the stratigraphic relationship between the three OSL samples from drill core # 13, although it is not part of the north-south transect across Dungeness foreland (see Fig 3 or 14 for core locations). The majority of samples are in stratigraphic order, including those from Camber Farm (#13), with the oldest OSL age obtained for each core being at the bottom of the core, and the youngest at the top. In some cases, the ages are consistent with each other, giving the same age within errors, and implying

rapid deposition of the sediment. There are few significant down-core age reversals – any discrepancies in the central OSL ages shown are accounted for within 2σ error between neighbouring samples down-core (eg cores 1, 2 and 5), with the exception of the sample from the bottom of core 8 (Fig 15b) which is discussed below. This means that for some cores, deposition is sufficiently rapid that the ages cannot be resolved, in spite of their high precision.

Table 7.1: OSL sample details, equivalent dose and dose rate data, and OSL ages – core 1.

	Deep drill core 1 – Broomhill Farm		
Aberystwyth Lab. number	**73 BH 1/1**	**73 BH 1/2**	**73 BH 1/3**
Altitude (m OD)	-0.89	-3.09	-5.19
Depth down-core (m)	3.75 ± 0.05	5.95 ± 0.05	8.05 ± 0.05
Material used for dating	Quartz		
Grain size (μm)	150-180	150-180	150-180
Preparation method	Heavy liquid separation (sodium polytungstate); 40% HF etch 45 mins		
Measurement protocol	SAR; OSL 470nm; detection filter 7.5mm Hoya U-340		
No. aliquots measured	48	48	24
No. aliquots used for D_e	31	33	18
Equivalent Dose, D_e (Gy)*	**3.70 ± 0.06**	**3.11 ± 0.05**	**3.44 ± 0.06**
Water content (% dry mass)	21 ± 5	24 ± 5	25 ± 5
Unsealed α count rate (cts/ks.cm^2)	0.162 ± 0.003	0.211 ± 0.004	0.221 ± 0.004
U (ppm)	0.82 ± 0.08	0.85 ± 0.10	1.33 ± 0.09
Th (ppm)	1.84 ± 0.24	3.11 ± 0.34	1.75 ± 0.27
α count rate Sealed/Unsealed	0.95 ± 0.03	0.96 ± 0.03	1.03 ± 0.04
Infinite β dose rate (Gy/ka)	0.584 ± 0.013	0.568 ± 0.008	0.512 ± 0.012
Calculated K (%)	0.53 ± 0.02	0.46 ± 0.03	0.35 ± 0.02
Layer removed by etching (μm)	10 ± 2	10 ± 2	10 ± 2
External β dose rate 'wet' (Gy/ka)	0.412 ± 0.023	0.389 ± 0.020	0.348 ± 0.019
External γ dose rate 'wet' (Gy/ka)	0.249 ± 0.017	0.279 ± 0.021	0.248 ± 0.017
Cosmic (Gy/ka)	0.126 ± 0.013	0.097 ± 0.010	0.077 ± 0.008
Total dose rate (Gy/ka)	**0.79 ± 0.03**	**0.77 ± 0.03**	**0.67 ± 0.03**
OSL Age#* (a)	**4700 ± 200**	**4070 ± 170**	**5120 ± 220**

Ages are expressed as years before 2000 AD, rounded to the nearest 10 years.
* The error shown following the D_e value is the standard error on the mean.

Table 7.2: OSL sample details, equivalent dose and dose rate data, and OSL ages – core 2.

	Deep drill core 2 – The Midrips		
Aberystwyth Lab. number	**73 BH 2/1**	**73 BH 2/2**	**73 BH 2/3**
Altitude (m OD)	-6.99	-7.99	-9.34
Depth down-core (m)	11.25 ± 0.05	12.25 ± 0.05	13.60± 0.05
Material used for dating	Quartz		
Grain size (μm)	150-180	150-180	150-180
Preparation method	Heavy liquid separation (sodium polytungstate); 40% HF etch 45 mins		
Measurement protocol	SAR; OSL 470nm; detection filter 7.5mm Hoya U-340		
No. aliquots measured	24	24	24
No. aliquots used for D_e	18	17	12
Equivalent Dose, D_e (Gy)*	**4.31 ± 0.09**	**3.81 ± 0.08**	**3.55 ± 0.09**
Water content (% dry mass)	25 ± 5	25 ± 5	25 ± 5
Unsealed α count rate (cts/ks.cm²)	0.298 ± 0.005	0.298 ± 0.005	0.163 ± 0.003
U (ppm)	1.27 ± 0.15	1.40 ± 0.14	0.73 ± 0.09
Th (ppm)	4.14 ± 0.49	3.71 ± 0.46	2.16 ± 0.27
α count rate Sealed/Unsealed	1.07 ± 0.03	0.97 ± 0.03	1.10 ± 0.04
Infinite β dose rate (Gy/ka)	0.724 ± 0.014	0.736 ± 0.015	0.746 ± 0.009
Calculated K (%)	0.54 ± 0.04	0.55 ± 0.04	0.74 ± 0.02
Layer removed by etching (μm)	10 ± 2	10 ± 2	10 ± 2
External β dose rate 'wet' (Gy/ka)	0.491 ± 0.025	0.500 ± 0.026	0.506 ± 0.025
External γ dose rate 'wet' (Gy/ka)	0.368 ± 0.029	0.365 ± 0.028	0.285 ± 0.018
Cosmic (Gy/ka)	0.056 ± 0.006	0.051 ± 0.005	0.046 ± 0.005
Total dose rate (Gy/ka)	**0.92 ± 0.04**	**0.92 ± 0.04**	**0.84 ± 0.03**
OSL Age#* (a)	**4710 ± 220**	**4170 ± 190**	**4240 ± 190**

Ages are expressed as years before 2000 AD, rounded to the nearest 10 years.
* The error shown following the D_e value is the standard error on the mean.

Table 7.3: OSL sample details, equivalent dose and dose rate data, and OSL ages – core 3.

	Deep drill core 3– The Forelands		
Aberystwyth Lab. number	**73 BH 3/1**	**73 BH 3/2**	**73 BH 3/3**
Altitude (m OD)	-8.47	-9.47	-11.32
Depth down-core (m)	12.90± 0.05	13.90± 0.05	15.75 ± 0.05
Material used for dating	Quartz		
Grain size (μm)	150-180	150-180	150-180
Preparation method	Heavy liquid separation (sodium polytungstate); 40% HF etch 45 mins		
Measurement protocol	SAR; OSL 470nm; detection filter 7.5mm Hoya U-340		
No. aliquots measured	24	24	24
No. aliquots used for D_e	17	18	17
Equivalent Dose, D_e (Gy)*	**2.37 ± 0.06**	**2.42 ± 0.06**	**3.73 ± 0.09**
Water content (% dry mass)	25 ± 5	25 ± 5	25 ± 5
Unsealed α count rate ($cts/ks.cm^2$)	0.130 ± 0.002	0.159 ± 0.003	0.292 ± 0.005
U (ppm)	0.58 ± 0.06	0.77 ± 0.08	1.59 ± 0.13
Th (ppm)	1.74 ± 0.20	1.90 ± 0.25	2.92 ± 0.41
α count rate Sealed/Unsealed	0.96 ± 0.03	1.00 ± 0.03	1.03 ± 0.04
Infinite β dose rate (Gy/ka)	0.566 ± 0.013	0.527 ± 0.012	0.767 ± 0.014
Calculated K (%)	0.56 ± 0.02	0.46 ± 0.02	0.58 ± 0.03
Layer removed by etching (μm)	10 ± 2	10 ± 2	10 ± 2
External β dose rate 'wet' (Gy/ka)	0.384 ± 0.020	0.357 ± 0.019	0.521 ± 0.027
External γ dose rate 'wet' (Gy/ka)	0.220 ± 0.014	0.226 ± 0.016	0.358 ± 0.025
Cosmic (Gy/ka)	0.049 ± 0.005	0.045 ± 0.005	0.038 ± 0.004
Total dose rate (Gy/ka)	**0.65 ± 0.03**	**0.63 ± 0.03**	**0.92 ± 0.04**
OSL Age#* (a)	**3630 ± 160**	**3850 ± 180**	**4070 ± 190**

Ages are expressed as years before 2000 AD, rounded to the nearest 10 years.
* The error shown following the D_e value is the standard error on the mean.

Table 7.4: OSL sample details, equivalent dose and dose rate data, and OSL ages – core 4.

	Deep drill core 4 – Holmstone		
Aberystwyth Lab. number	**73 BH 4/1**	**73 BH 4/2**	**73 BH 4/3**
Altitude (m OD)	-5.46	-7.06	-10.06
Depth down-core (m)	9.95 ± 0.05	11.55 ± 0.05	14.55 ± 0.05
Material used for dating	Quartz		
Grain size (μm)	150-180	150-180	125-150
Preparation method	Heavy liquid separation (sodium polytungstate); 40% HF etch 45 mins		
Measurement protocol	SAR; OSL 470nm; detection filter 7.5mm Hoya U-340		
No. aliquots measured	21	21	21
No. aliquots used for D_e	17	18	13
Equivalent Dose, D_e (Gy)*	**1.34 ± 0.03**	**1.75 ± 0.04**	**2.30 ± 0.05**
Water content (% dry mass)	25 ± 5	25 ± 5	25 ± 5
Unsealed α count rate (cts/ks.cm^2)	0.220 ± 0.004	0.273 ± 0.005	0.197 ± 0.003
U (ppm)	1.00 ± 0.11	1.23 ± 0.14	0.88 ± 0.09
Th (ppm)	2.86 ± 0.35	3.60 ± 0.44	2.61 ± 0.30
α count rate Sealed/Unsealed	0.99 ± 0.03	1.06 ± 0.03	0.99 ± 0.04
Infinite β dose rate (Gy/ka)	0.578 ± 0.013	0.593 ± 0.013	0.806 ± 0.015
Calculated K (%)	0.45 ± 0.03	0.40 ± 0.03	0.78 ± 0.03
Layer removed by etching (μm)	10 ± 2	10 ± 2	10 ± 2
External β dose rate 'wet' (Gy/ka)	0.392 ± 0.021	0.403 ± 0.021	0.553 ± 0.028
External γ dose rate 'wet' (Gy/ka)	0.279 ± 0.021	0.318 ± 0.026	0.321 ± 0.021
Cosmic (Gy/ka)	0.064 ± 0.006	0.055 ± 0.006	0.042 ± 0.004
Total dose rate (Gy/ka)	**0.74 ± 0.03**	**0.78 ± 0.03**	**0.92 ± 0.04**
OSL Age#* (a)	**1830 ± 90**	**2260 ± 110**	**2510 ± 110**

Ages are expressed as years before 2000 AD, rounded to the nearest 10 years.
* The error shown following the D_e value is the standard error on the mean.

Table 7.5: OSL sample details, equivalent dose and dose rate data, and OSL ages – core 5.

	Deep drill core 5 – South Brooks	
Aberystwyth Lab. number	**73 BH 5/1**	**73 BH 5/2**
Altitude (m OD)	-6.45	-7.40
Depth down-core (m)	9.90 ± 0.05	10.85 ± 0.05
Material used for dating	Quartz	
Grain size (μm)	150-180	150-180
Preparation method	Heavy liquid separation (sodium polytungstate); 40% HF etch 45 mins	
Measurement protocol	SAR; OSL 470nm; detection filter 7.5mm Hoya U-340	
No. aliquots measured	21	21
No. aliquots used for D_e	19	18
Equivalent Dose, D_e (Gy)*	**1.41 ± 0.04**	**1.39 ± 0.04**
Water content (% dry mass)	25 ± 5	25 ± 5
Unsealed α count rate (cts/ks.cm^2)	0.144 ± 0.003	0.142 ± 0.003
U (ppm)	0.73 ± 0.07	0.64 ± 0.07
Th (ppm)	1.59 ± 0.21	1.86 ± 0.23
α count rate Sealed/Unsealed	0.99 ± 0.03	0.98 ± 0.03
Infinite β dose rate (Gy/ka)	0.608 ± 0.013	0.682 ± 0.014
Calculated K (%)	0.59 ± 0.02	0.69 ± 0.02
Layer removed by etching (μm)	10 ± 2	10 ± 2
External β dose rate 'wet' (Gy/ka)	0.413 ± 0.022	0.463 ± 0.024
External γ dose rate 'wet' (Gy/ka)	0.234 ± 0.015	0.255 ± 0.016
Cosmic (Gy/ka)	0.064 ± 0.006	0.058 ± 0.006
Total dose rate (Gy/ka)	**0.71 ± 0.03**	**0.78 ± 0.03**
OSL Age#* (a)	**1990 ± 100**	**1790 ± 80**

Ages are expressed as years before 2000 AD, rounded to the nearest 10 years.
* The error shown following the D_e value is the standard error on the mean.

Table 7.6: OSL sample details, equivalent dose and dose rate data, and OSL ages – core 6.

	Deep drill core 6 – Dungeness Road Gate		
Aberystwyth Lab. number	**73 BH 6/1**	**73 BH 6/2**	**73 BH 6/3**
Altitude (m OD)	-6.36	-9.26	-10.41
Depth down-core (m)	10.65 ± 0.05	13.55 ± 0.05	14.70 ± 0.05
Material used for dating	Quartz		
Grain size (μm)	150-180	150-180	150-180
Preparation method	Heavy liquid separation (sodium polytungstate); 40% HF etch 45 mins		
Measurement protocol	SAR; OSL 470nm; detection filter 7.5mm Hoya U-340		
No. aliquots measured	24	24	48
No. aliquots used for D_e	14	15	26
Equivalent Dose, D_e (Gy)*	**1.10 ± 0.02**	**1.40 ± 0.05**	**1.55 ± 0.03**
Water content (% dry mass)	25 ± 5	25 ± 5	25 ± 5
Unsealed α count rate ($cts/ks.cm^2$)	0.127 ± 0.002	0.224 ± 0.003	0.316 ± 0.006
U (ppm)	0.54 ± 0.06	1.12 ± 0.09	1.48 ± 0.15
Th (ppm)	1.76 ± 0.20	2.58 ± 0.30	3.98 ± 0.50
α count rate Sealed/Unsealed	0.97 ± 0.03	1.03 ± 0.03	1.03 ± 0.03
Infinite β dose rate (Gy/ka)	0.461 ± 0.012	0.566 ± 0.013	0.609 ± 0.013
Calculated K (%)	0.43 ± 0.02	0.43 ± 0.03	0.36 ± 0.04
Layer removed by etching (μm)	10 ± 2	10 ± 2	10 ± 2
External β dose rate 'wet' (Gy/ka)	0.313 ± 0.017	0.384 ± 0.020	0.413 ± 0.022
External γ dose rate 'wet' (Gy/ka)	0.194 ± 0.013	0.274 ± 0.019	0.346 ± 0.028
Cosmic (Gy/ka)	0.059 ± 0.006	0.046 ± 0.005	0.042 ± 0.004
Total dose rate (Gy/ka)	**0.57 ± 0.02**	**0.70 ± 0.03**	**0.80 ± 0.04**
OSL Age#* (a)	**1940 ± 80**	**1990 ± 100**	**1930 ± 100**

Ages are expressed as years before 2000 AD, rounded to the nearest 10 years.
* The error shown following the D_e value is the standard error on the mean.

Table 7.7: OSL sample details, equivalent dose and dose rate data, and OSL ages – core 7.

	Deep drill core 7 – Dengemarsh Road		
Aberystwyth Lab. number	**73 BH 7/1**	**73 BH 7/2**	**73 BH 7/3**
Altitude (m OD)	-6.16	-8.41	-10.56
Depth down-core (m)	10.30 ± 0.05	12.55 ± 0.05	14.70 ± 0.05
Material used for dating	Quartz		
Grain size (μm)	125-150	125-150	125-150
Preparation method	Heavy liquid separation (sodium polytungstate); 40% HF etch 45 mins		
Measurement protocol	SAR; OSL 470nm; detection filter 7.5mm Hoya U-340		
No. aliquots measured	21	21	42
No. aliquots used for D_e	12	14	29
Equivalent Dose, D_e (Gy)*	**1.18 ± 0.02**	**1.17 ± 0.04**	**1.20 ± 0.03**
Water content (% dry mass)	25 ± 5	25 ± 5	25 ± 5
Unsealed α count rate ($cts/ks.cm^2$)	0.302 ± 0.005	0.241 ± 0.004	0.220 ± 0.004
U (ppm)	1.50 ± 0.14	1.13 ± 0.10	0.72 ± 0.12
Th (ppm)	3.48 ± 0.44	3.02 ± 0.32	3.82 ± 0.40
α count rate Sealed/Unsealed	1.00 ± 0.017	0.98 ± 0.03	0.96 ± 0.03
Infinite β dose rate (Gy/ka)	1.025 ± 0.017	0.694 ± 0.014	0.656 ± 0.014
Calculated K (%)	0.91 ± 0.04	0.57 ± 0.03	0.57 ± 0.03
Layer removed by etching (μm)	10 ± 2	10 ± 2	10 ± 2
External β dose rate 'wet' (Gy/ka)	0.704 ± 0.036	0.477 ± 0.025	0.450 ± 0.023
External γ dose rate 'wet' (Gy/ka)	0.433 ± 0.029	0.319 ± 0.021	0.313 ± 0.024
Cosmic (Gy/ka)	0.061 ± 0.006	0.050 ± 0.005	0.042 ± 0.004
Total dose rate (Gy/ka)	**1.20 ± 0.05**	**0.85 ± 0.03**	**0.81 ± 0.03**
OSL Age#* (a)	**980 ± 40**	**1390 ± 70**	**1500 ± 70**

Ages are expressed as years before 2000 AD, rounded to the nearest 10 years.
* The error shown following the D_e value is the standard error on the mean.

Table 7.8: OSL sample details, equivalent dose and dose rate data, and OSL ages – core 8.

	Deep drill core 8 – Dungeness Lookout		
Aberystwyth Lab. number	**73 BH 8/1**	**73 BH 8/2**	**73 BH 8/3**
Altitude (m OD)	-12.09	-8.84	-15.48
Depth down-core (m)	17.25 ± 0.05	14.00 ± 0.04	21.00 ± 0.05
Material used for dating	Quartz		
Grain size (μm)	150-180	150-180	150-180
Preparation method	Heavy liquid separation (sodium polytungstate); 40% HF etch 45 mins		
Measurement protocol	SAR; OSL 470nm; detection filter 7.5mm Hoya U-340		
No. aliquots measured	21	21	21
No. aliquots used for D_e	15	13	14
Equivalent Dose, D_e (Gy)*	**0.78 ± 0.03**	**0.65 ± 0.02**	**0.91 ± 0.03**
Water content (% dry mass)	25 ± 5	25 ± 5	25 ± 5
Unsealed α count rate (cts/ks.cm^2)	0.113 ± 0.002	0.115 ± 0.002	0.325 ± 0.006
U (ppm)	0.53 ± 0.06	0.60 ± 0.05	1.44 ± 0.17
Th (ppm)	1.41 ± 0.18	1.25 ± 0.17	4.36 ± 0.55
α count rate Sealed/Unsealed	1.08 ± 0.04	1.07 ± 0.04	1.01 ± 0.03
Infinite β dose rate (Gy/ka)	0.510 ± 0.013	0.417 ± 0.011	1.092 ± 0.011
Calculated K (%)	0.50 ± 0.02	0.38 ± 0.02	0.98 ± 0.04
Layer removed by etching (μm)	10 ± 2	10 ± 2	10 ± 2
External β dose rate 'wet' (Gy/ka)	0.346 ± 0.019	0.283 ± 0.016	0.741 ± 0.036
External γ dose rate 'wet' (Gy/ka)	0.194 ± 0.013	0.170 ± 0.012	0.473 ± 0.034
Cosmic (Gy/ka)	0.034 ± 0.003	0.044 ± 0.004	0.026 ± 0.003
Total dose rate (Gy/ka)	**0.57 ± 0.02**	**0.50 ± 0.02**	**1.24 ± 0.05**
OSL Age#* (a)	**1360 ± 70**	**1300 ± 70**	**740 ± 40**

Ages are expressed as years before 2000 AD, rounded to the nearest 10 years.
* The error shown following the D_e value is the standard error on the mean.

Table 7.9: OSL sample details, equivalent dose and dose rate data, and OSL ages – core 9.

	Deep drill core 9 – RSPB Visitor Centre		
Aberystwyth Lab. number	**73 BH 9/1**	**73 BH 9/2**	**73 BH 9/3**
Altitude (m OD)	-1.72	-4.22	-6.02
Depth down-core (m)	4.85 ± 0.05	7.35 ± 0.05	9.15 ± 0.05
Material used for dating	Quartz		
Grain size (μm)	180-212	150-180	150-180
Preparation method	Heavy liquid separation (sodium polytungstate); 40% HF etch 45 mins		
Measurement protocol	SAR; OSL 470nm; detection filter 7.5mm Hoya U-340		
No. aliquots measured	21	21	21
No. aliquots used for D_e	15	17	14
Equivalent Dose, D_e (Gy)*	**0.60 ± 0.03**	**1.04 ± 0.03**	**1.03 ± 0.03**
Water content (% dry mass)	25 ± 5	25 ± 5	25 ± 5
Unsealed α count rate (cts/ks.cm^2)	0.109 ± 0.002	0.238 ± 0.004	0.328 ± 0.006
U (ppm)	0.51 ± 0.05	1.18 ± 0.12	1.71 ± 0.15
Th (ppm)	1.39 ± 0.17	2.76 ± 0.37	3.53 ± 0.47
α count rate Sealed/Unsealed	1.12 ± 0.04	1.00 ± 0.03	1.00 ± 0.03
Infinite β dose rate (Gy/ka)	0.434 ± 0.011	0.844 ± 0.016	0.839 ± 0.009
Calculated K (%)	0.41 ± 0.02	0.76 ± 0.03	0.63 ± 0.03
Layer removed by etching (μm)	10 ± 2	10 ± 2	10 ± 2
External β dose rate 'wet' (Gy/ka)	0.290 ± 0.016	0.572 ± 0.029	0.569 ± 0.028
External γ dose rate 'wet' (Gy/ka)	0.174 ± 0.012	0.350 ± 0.024	0.401 ± 0.029
Cosmic (Gy/ka)	0.110 ± 0.011	0.083 ± 0.008	0.069 ± 0.007
Total dose rate (Gy/ka)	**0.57 ± 0.02**	**1.01 ± 0.04**	**1.04 ± 0.04**
OSL Age#* (a)	**1050 ± 70**	**1040 ± 50**	**990 ± 50**

Ages are expressed as years before 2000 AD, rounded to the nearest 10 years.
* The error shown following the D_e value is the standard error on the mean.

Table 7.10: OSL sample details, equivalent dose and dose rate data, and OSL ages – core 10.

	Deep drill core 10 – ARC		
Aberystwyth Lab. number	**73 BH 10/1**	**73 BH 10/2**	**73 BH 10/3**
Altitude (m OD)	-1.94	-3.94	-5.84
Depth down-core (m)	5.85 ± 0.05	7.85 ± 0.05	9.75 ± 0.05
Material used for dating	Quartz		
Grain size (μm)	150-180	150-180	150-180
Preparation method	Heavy liquid separation (sodium polytungstate); 40% HF etch 45 mins		
Measurement protocol	SAR; OSL 470nm; detection filter 7.5mm Hoya U-340		
No. aliquots measured	72	48	29
No. aliquots used for D_e	44	27	20
Equivalent Dose, D_e (Gy)*	**0.56 ± 0.01**	**0.71 ± 0.01**	**1.24 ± 0.03**
Water content (% dry mass)	25 ± 5	25 ± 5	25 ± 5
Unsealed α count rate (cts/ks.cm^2)	0.088 ± 0.002	0.243 ± 0.004	0.323 ± 0.005
U (ppm)	0.48 ± 0.04	1.28 ± 0.11	1.71 ± 0.14
Th (ppm)	0.86 ± 0.13	2.56 ± 0.35	3.37 ± 0.44
α count rate Sealed/Unsealed	1.12 ± 0.04	0.97 ± 0.03	0.98 ± 0.03
Infinite β dose rate (Gy/ka)	0.457 ± 0.015	0.563 ± 0.013	1.031 ± 0.017
Calculated K (%)	0.46 ± 0.02	0.39 ± 0.03	0.88 ± 0.04
Layer removed by etching (μm)	10 ± 2	10 ± 2	10 ± 2
External β dose rate 'wet' (Gy/ka)	0.310 ± 0.018	0.382 ± 0.020	0.699 ± 0.035
External γ dose rate 'wet' (Gy/ka)	0.162 ± 0.010	0.282 ± 0.021	0.442 ± 0.029
Cosmic (Gy/ka)	0.098 ± 0.010	0.079 ± 0.008	0.065 ± 0.007
Total dose rate (Gy/ka)	**0.57 ± 0.02**	**0.74 ± 0.03**	**1.21 ± 0.05**
OSL Age#* (a)	**980 ± 40**	**960 ± 40**	**1030 ± 50**

Ages are expressed as years before 2000 AD, rounded to the nearest 10 years.
* The error shown following the D_e value is the standard error on the mean.

Table 7.11: OSL sample details, equivalent dose and dose rate data, and OSL ages – core 11.

	Deep drill core 11 – Greatstone		
Aberystwyth Lab. number	**73 BH 11/1**	**73 BH 11/2**	**73 BH 11/3**
Altitude (m OD)	1.25	-1.45	-3.70
Depth down-core (m)	1.80 ± 0.05	4.50 ± 0.05	6.75 ± 0.05
Material used for dating	Quartz		
Grain size (μm)	150-180	150-180	150-180
Preparation method	Heavy liquid separation (sodium polytungstate); 40% HF etch 45 mins		
Measurement protocol	SAR; OSL 470nm; detection filter 7.5mm Hoya U-340		
No. aliquots measured	42	21	21
No. aliquots used for D_e	35	12	14
Equivalent Dose, D_e (Gy)*	**0.35 ± 0.01**	**0.46 ± 0.02**	**0.81 ± 0.03**
Water content (% dry mass)	23 ± 5	25 ± 5	25 ± 5
Unsealed α count rate ($cts/ks.cm^2$)	0.134 ± 0.002	0.237 ± 0.004	0.327 ± 0.005
U (ppm)	0.69 ± 0.06	1.08 ± 0.12	1.46 ± 0.15
Th (ppm)	1.46 ± 0.19	3.08 ± 0.39	4.35 ± 0.47
α count rate Sealed/Unsealed	(unsealed meas. only)	1.01 ± 0.04	0.99 ± 0.03
Infinite β dose rate (Gy/ka)	0.614 ± 0.013	0.698 ± 0.014	0.691 ± 0.014
Calculated K (%)	0.61 ± 0.02	0.58 ± 0.03	0.46 ± 0.04
Layer removed by etching (μm)	10 ± 2	10 ± 2	10 ± 2
External β dose rate 'wet' (Gy/ka)	0.425 ± 0.023	0.474 ± 0.025	0.469 ± 0.024
External γ dose rate 'wet' (Gy/ka)	0.233 ± 0.014	0.319 ± 0.024	0.376 ± 0.028
Cosmic (Gy/ka)	0.162 ± 0.016	0.115 ± 0.012	0.088 ± 0.009
Total dose rate (Gy/ka)	**0.82 ± 0.03**	**0.91 ± 0.04**	**0.93 ± 0.04**
OSL Age#* (a)	**430 ± 20**	**510 ± 30**	**870 ± 50**

Ages are expressed as years before 2000 AD, rounded to the nearest 10 years.
* The error shown following the D_e value is the standard error on the mean.

Table 7.12: OSL sample details, equivalent dose and dose rate data, and OSL ages – core 12.

	Deep drill core 12 – Power Station		
Aberystwyth Lab. number	**73 BH 12/1**	**73 BH 12/2**	**73 BH 12/3**
Altitude (m OD)	-9.51	-9.96	-10.41
Depth down-core (m)	15.05 ± 0.05	15.50 ± 0.05	15.95 ± 0.05
Material used for dating	Quartz		
Grain size (μm)	150-180	150-180	150-180
Preparation method	Heavy liquid separation (sodium polytungstate); 40% HF etch 45 mins		
Measurement protocol	SAR; OSL 470nm; detection filter 7.5mm Hoya U-340		
No. aliquots measured	42	21	21
No. aliquots used for D_e	32	14	15
Equivalent Dose, D_e (Gy)*	**0.51 ± 0.01**	**0.46 ± 0.01**	**0.47 ± 0.02**
Water content (% dry mass)	25 ± 5	25 ± 5	25 ± 5
Unsealed α count rate (cts/ks.cm^2)	0.205 ± 0.004	0.223 ± 0.004	0.187 ± 0.003
U (ppm)	0.97 ± 0.10	1.16 ± 0.11	0.84 ± 0.09
Th (ppm)	2.54 ± 0.33	2.40 ± 0.34	2.46 ± 0.29
α count rate Sealed/Unsealed	1.05 ± 0.03	1.09 ± 0.04	1.03 ± 0.03
Infinite β dose rate (Gy/ka)	0.629 ± 0.014	0.627 ± 0.013	0.562 ± 0.013
Calculated K (%)	0.53 ± 0.03	0.50 ± 0.03	0.48 ± 0.03
Layer removed by etching (μm)	10 ± 2	10 ± 2	10 ± 2
External β dose rate 'wet' (Gy/ka)	0.426 ± 0.022	0.425 ± 0.022	0.381 ± 0.020
External γ dose rate 'wet' (Gy/ka)	0.280 ± 0.020	0.286 ± 0.021	0.255 ± 0.018
Cosmic (Gy/ka)	0.041 ± 0.004	0.039 ± 0.004	0.038 ± 0.004
Total dose rate (Gy/ka)	**0.75 ± 0.03**	**0.75 ± 0.03**	**0.67 ± 0.03**
OSL Age#* (a)	**680 ± 30**	**610 ± 30**	**700 ± 40**

Ages are expressed as years before 2000 AD, rounded to the nearest 10 years.
* The error shown following the D_e value is the standard error on the mean.

Table 7.13: OSL sample details, equivalent dose and dose rate data, and OSL ages – core 13.

	Deep drill core 13 – Castle Farm		
Aberystwyth Lab. number	**73 BH 13/1**	**73 BH 13/2**	**73 BH 13/3**
Altitude (m OD)	-5.04	-6.85	-7.95
Depth down-core (m)	9.57 ± 0.05	11.38 ± 0.05	12.48 ± 0.05
Material used for dating	Quartz		
Grain size (μm)	150-180	150-180	180-212
Preparation method	Heavy liquid separation (sodium polytungstate); 40% HF etch 45 mins		
Measurement protocol	SAR; OSL 470nm; detection filter 7.5mm Hoya U-340		
No. aliquots measured	42	21	21
No. aliquots used for D_e	24	14	15
Equivalent Dose, D_e (Gy)*	**0.76 ± 0.02**	**0.88 ± 0.04**	**1.10 ± 0.06**
Water content (% dry mass)	25 ± 5	25 ± 5	25 ± 5
Unsealed α count rate (cts/ks.cm²)	0.413 ± 0.007	0.370 ± 0.007	0.424 ± 0.007
U (ppm)	1.78 ± 0.20	1.59 ± 0.19	1.97 ± 0.19
Th (ppm)	5.71 ± 0.64	5.14 ± 0.62	5.37 ± 0.63
α count rate Sealed/Unsealed	1.05 ± 0.04	1.00 ± 0.03	0.97 ± 0.02
Infinite β dose rate (Gy/ka)	0.994 ± 0.017	0.776 ± 0.015	0.934 ± 0.016
Calculated K (%)	0.74 ± 0.05	0.52 ± 0.05	0.64 ± 0.05
Layer removed by etching (μm)	10 ± 2	10 ± 2	10 ± 2
External β dose rate 'wet' (Gy/ka)	0.674 ± 0.034	0.527 ± 0.027	0.625 ± 0.032
External γ dose rate 'wet' (Gy/ka)	0.507 ± 0.038	0.428 ± 0.035	0.493 ± 0.037
Cosmic (Gy/ka)	0.066 ± 0.007	0.056 ± 0.006	0.050 ± 0.005
Total dose rate (Gy/ka)	**1.25 ± 0.05**	**1.01 ± 0.05**	**1.17 ± 0.05**
OSL Age#* (a)	**610 ± 30**	**870 ± 60**	**940 ± 70**

Ages are expressed as years before 2000 AD, rounded to the nearest 10 years.
* The error shown following the D_e value is the standard error on the mean.

Table 7.14: OSL sample details, equivalent dose and dose rate data, and OSL ages – core MP1.

	Short hand-core – Moneypenny Farm
Aberystwyth Lab. number	**80 MP 1**
Altitude (m OD)	1.6
Depth down-core (m)	2.27 ± 0.05
Material used for dating	Quartz
Grain size (μm)	150-180
Preparation method	Heavy liquid separation (sodium polytungstate); 40% HF etch 45 mins
Measurement protocol	SAR; OSL 470nm; detection filter 7.5mm Hoya U-340
No. aliquots measured	26
No. aliquots used for D_e	19
Equivalent Dose, D_e (Gy)*	**0.29 ± 0.01**
Water content (% dry mass)	23 ± 5
Unsealed α count rate (cts/ks.cm^2)	0.093 ± 0.002
U (ppm)	0.39 ± 0.05
Th (ppm)	1.32 ± 0.16
α count rate Sealed/Unsealed	0.96 ± 0.04
Infinite β dose rate (Gy/ka)	0.378 ± 0.007
Calculated K (%)	0.37 ± 0.01
Layer removed by etching (μm)	10 ± 2
External β dose rate 'wet' (Gy/ka)	0.258 ± 0.013
External γ dose rate 'wet' (Gy/ka)	0.155 ± 0.011
Cosmic (Gy/ka)	0.152 ± 0.015
Total dose rate (Gy/ka)	**0.56 ± 0.02**
OSL Age#* (a)	**510 ± 30**

Ages are expressed as years before 2000 AD, rounded to the nearest 10 years.
* The error shown following the D_e value is the standard error on the mean.

Table 7.15: OSL sample details, equivalent dose and dose rate data, and OSL ages.

Modern analogue surface samples – Greatstone Beach		
Aberystwyth Lab. number	**73 BH USS**	**73 BH SSR**
Sample description	Upper shoreface sands	Symmetrical sand ripples
Depth down-core (m)	0.00 ± 0.01	0.00 ± 0.01
Material used for dating	Quartz	
Grain size (μm)	150-180	150-180
Preparation method	Heavy liquid separation (sodium polytungstate); 40% HF etch 45 mins	
Measurement protocol	SAR; OSL 470nm; detection filter 7.5mm Hoya U-340	
No. aliquots measured	18	13
No. aliquots used for D_e	12	11
Equivalent Dose, D_e (Gy)*	**0.03 ± 0.03**	**0.02 ± 0.02**
Water content (% dry mass)	25 ± 5	25 ± 5
Unsealed α count rate (cts/ks.cm^2)	0.093 ± 0.001	0.308 ± 0.005
U (ppm)	0.52 ± 0.03	1.47 ± 0.14
Th (ppm)	0.88 ± 0.11	3.79 ± 0.44
α count rate Sealed/Unsealed	1.02 ± 0.04	0.99 ± 0.03
Infinite β dose rate (Gy/ka)	0.448 ± 0.007	0.719 ± 0.015
Calculated K (%)	0.45 ± 0.01	0.51 ± 0.04
Layer removed by etching (μm)	10 ± 2	10 ± 2
External β dose rate 'wet' (Gy/ka)	0.304 ± 0.015	0.488 ± 0.025
External γ dose rate 'wet' (Gy/ka)	0.163 ± 0.009	0.366 ± 0.027
Cosmic (Gy/ka)	0.292 ± 0.029	0.292 ± 0.029
Total dose rate (Gy/ka)	**0.76 ± 0.03**	**1.15 ± 0.05**
OSL Age# (a)	**40 ± 40**	**15 ± 15**

Ages are expressed as years before 2000 AD, rounded to the nearest 5 years.
* The error shown is the standard deviation on the mean.

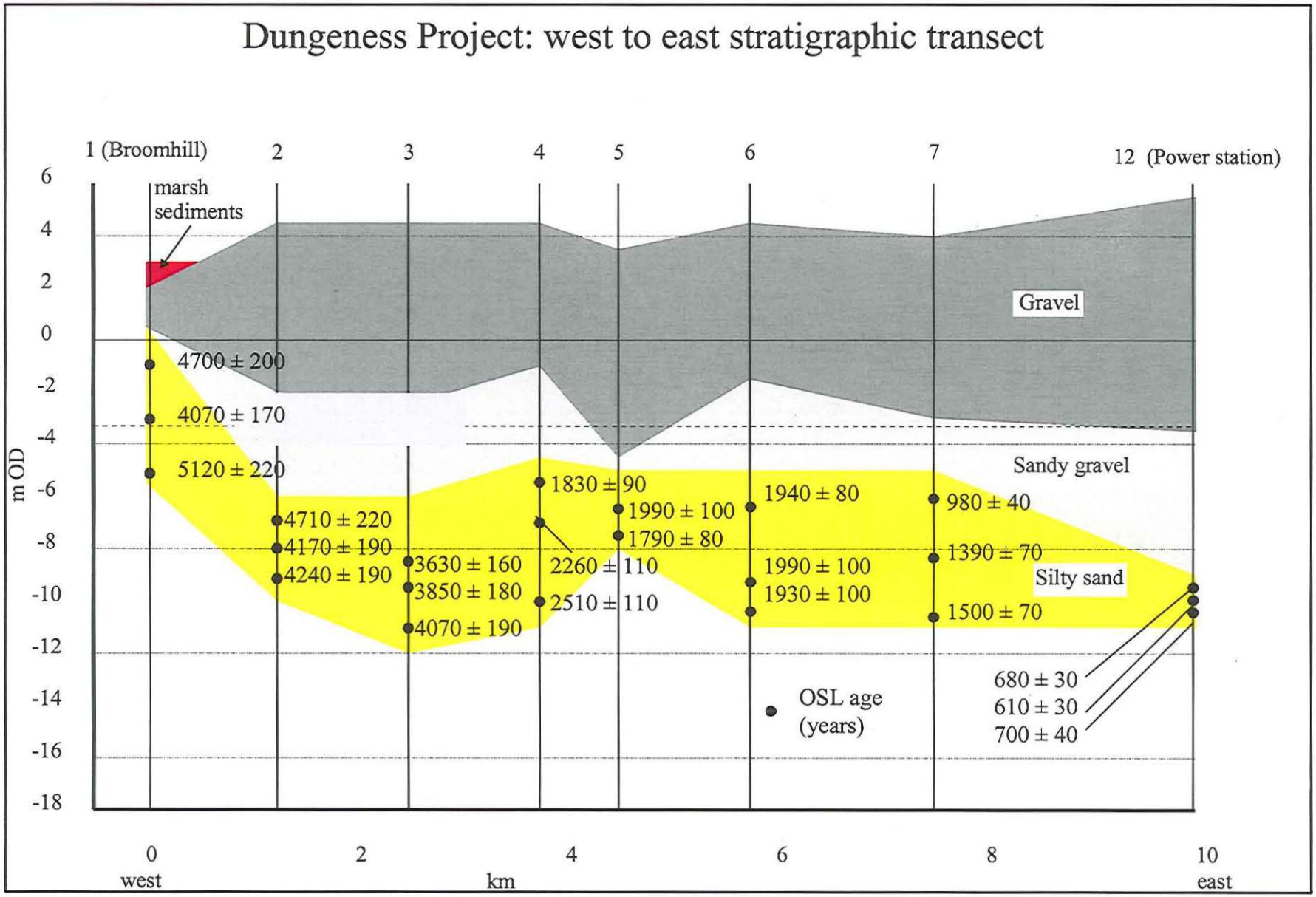

Figure 15a: OSL ages of samples from the west – east stratigraphic transect across the Dungeness Foreland.

Figure 15b: OSL ages of samples from the north-south stratigraphic transect across the Dungeness Foreland, plus the Camber Farm drill core (Rye project).

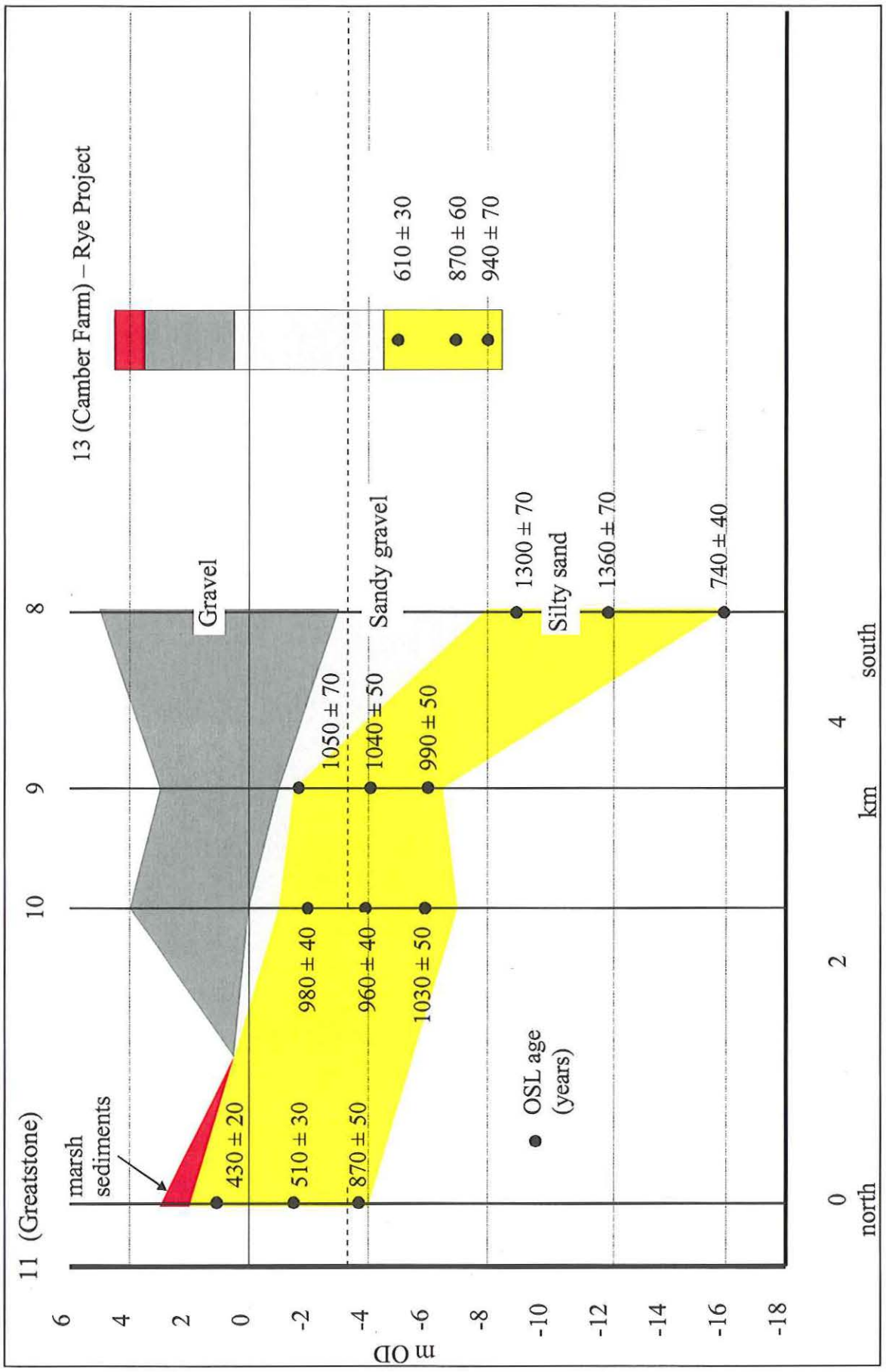

Core 8 shows a significant down-core age discrepancy, which cannot be accounted for within errors. Reassuringly, the D_e values obtained for the samples from core 8 increase in magnitude down-core, being approximately 0.7, 0.8, and 0.9 Gy for sample numbers 2 (top), 1 (middle), and 3 (bottom), respectively (Table 7.8). This increase in D_e value down-core is to be expected for what appears visually to be a homogenous silty-sand unit, with the increase in D_e for older samples at the bottom of the core reflecting the increased duration of exposure to naturally occurring ionising radiation. The dose rate for the upper two samples from core 8 is similar, being 0.50 and 0.57 Gy/ka for the top and middle samples, respectively (Table 7.8). However, the dose rate for sample 3 is more than twice that of the other two samples from this core, being 1.24 Gy/ka. This higher dose rate is reflected in both the alpha and beta counting data, suggesting that these data are sound. The uranium to thorium ratios are reasonable for all three samples (being 1:2.1, 1:2.7, and 1:3.0 for the top, middle, and bottom samples, respectively), suggesting again that the laboratory determinations of the dose rates for the sample material measured is sound.

Considering the D_e and dose rate information for core 8, it appears that the OSL age of sample 73BH-8/3, from the bottom the core, is erroneously young; it is not in stratigraphic agreement with the two OSL ages for samples taken from above it, which are believed to be sound. Whilst the laboratory dosimetry measurements made for subsamples of the material surrounding the ~10cm long OSL sample are believed to be sound, the discrepancy between the D_e and age data for core 8 suggest that the dosimetry subsample taken for the bottom sample, 73BH-8/3, does not accurately represent the 30cm diameter field of radiation contributing to the dose rate received by the sample during burial. Whilst the silty sand unit sampled appeared homogenous to the naked eye, it may be that the lowermost sample was taken from a zone which had a localised increase in the proportion of fine-grained material, thus causing a high dose rate to be measured around the OSL sample itself, but with a lower dose rate contribution being made to the OSL sample further from the sample location, due to the presence of coarser material. Indeed, examination of the particle size data collected during OSL sample preparation (Table 8) shows that sample 73BH-8/3 is very poorly sorted compared to the other two samples from that core, having a high proportion of both very coarse (31% >250 μm) and fine (16% <90 μm) material.

Table 8: Percentage mass of sediment in various particle size ranges.

Particle size range	% mass sediment in particle size range		
	BH 8/1	BH 8/2	BH 8/3
>250 µm	3.9	8.3	30.9
212-250 µm	19.7	12.0	4.6
180-212 µm	25.4	24.6	14.2
150-180 µm	30.3	38.5	11.6
125-150 µm	12.8	12.9	11.6
90-125 µm	5.7	2.5	10.9
<90 µm	2.2	1.2	16.2

If a dose rate more consistent with that of the uppermost two samples from core 8 is used for the bottom sample, the age calculated is then significantly older than that of the other samples from core 8. Whilst this practice is not recommended for the determination of the age of this sample, the exercise is offered as supporting evidence that some error lies in the determination of the dose rate received by sample 73BH-8/3.

The large number of OSL samples taken from the sub-gravel sand unit, both at various depths down-core, and also in transects across the landscape, permits the study of rates of deposition and progradation of the sand body underlying the gravel foreland at Dungeness (cores 1-12). Where the OSL ages down-core all agree within 1σ error, the ages must be considered to be equal and therefore deposition of the silty-sand unit at that location must be considered essentially 'instantaneous'. This is the case for all samples in cores 6, 9, 10 and the two acceptable uppermost ages from core 8, discussed above (see Figs 15a and b). This agreement in ages down-core does not appear to be a reflection of the sampling interval, thickness of sediment between samples or length of core (see Figs 15a and b), or necessarily a function of the age of the material. Rather, it is a reflection of either a true change in deposition rates at these sites (cores 6, 8, 9 and 10 - Fig 14) around 1900 – 1000 years ago (Figs 15a and b), compared to other sites sampled, or else it is an artefact of sampling along transects which run across a feature where the direction of growth and development changes over time and, hence, distance. At the other extreme, cores 4 and 11 show an increase in the mean OSL age down-core, with all OSL ages from each core being discrete even when 1σ errors are considered. Here, deposition is occurring sufficiently slowly to enable the OSL ages to resolve the deposition rate through the whole of the silty sand unit sampled; alternatively, this might again be a function of sampling. These issues are discussed further in section 9.

Taking three OSL samples per core along two perpendicular transects across the foreland offers reassurance of the stratigraphic integrity of the samples, and enables lateral as well as vertical comparsions of the OSL age data to be made. Such a detailed study minimises the effect any outliers may have on

understanding the development of the feature in question. Having considered the spatial relationship between OSL ages of the uppermost samples (Fig 14) and also the vertical stratigraphic relationship of the samples taken from each core (Figs 15a and b) to identify any potential outliers to the data (from which only one serious discrepancy was identified, ie 73BH-8/3), the relationship between all OSL ages across the foreland (cores 1-12) can now be considered, in section 9.

9. Discussion and interpretation of the OSL ages

9.1 Dungeness Foreland

Nature, Rate and Direction of Sand Body Progradation

Figures 16a and b consider hypothetical lines of equal age ('isochrons') linking the sub-gravel sand samples from the two transects of deep-drill cores taken across the Dungeness foreland (cores 1-12). The OSL age data are indicative of sigmoidal isochrones, which may represent a sequence of former shoreface/intertidal surfaces as the foreland precursor prograded eastward. These sigmoidal isochrons decrease in altitude from west to east (Transect 1-12 shown on Fig 14) and from north to south (Transect 8-11 shown on Fig 14), implying that the sand body developed eastward over the period from ~5000-400 years ago as an elongated foreland or spit-like environment, with the shore sloping away to the north, east and south. This interpretation, as well as the apparent sigmoidal form of the isochrons, agrees well with nearshore seismic survey evidence of a seaward-prograding shelf sand body (Dix *et al* 1998).

Although these isochrons cannot be located quantitatively on either cross-section (Figs 16a and b), their general spacing is indicative of an increase in progradation rate, ie spacing increases from west to east on Transect 1-12 (Fig 16a). This is especially the case after about 2000 years ago, during which time the sub-gravel sand supported the progradation of Dungeness Foreland from the region of core 6 to the present shoreline. Isochron spacing may also appear to increase for the period from ~1300-500 years ago in a northward direction along Transect 8-11 (Fig 16b).

These chronological data may be interpreted as an increase in sand body progradation rate through time, with the first evidence of an increase dating from approximately 2000 years ago. However, this interpretation assumes that the axis of progradation runs parallel to the direction of the transects. The observed pattern of age data may equally be explained by a constant rate of sand body development, but with the direction of extension being more oblique to the direction of Transect 1-12 during the period from 5000-2000 years ago, becoming progressively more parallel during the last 2000 years. This second model is in good correspondence with the orientation of the overlying gravel storm beaches, orthogonals which rotate from being more south-eastward to north-eastward between Broomhill (core 1) and Dungeness Road (core 7) - corresponding to the deposition of the underlying sand body between ~5000 to 1000 years ago. Hence, the apparent temporal trend in progradation rate may be a simple function of the sampling transect becoming progressively more aligned with the axis of foreland development. A similar temporal change in isochron spacing for Transect 8-11 is not clearly expressed, particularly as there is also an underlying altitudinal trend here.

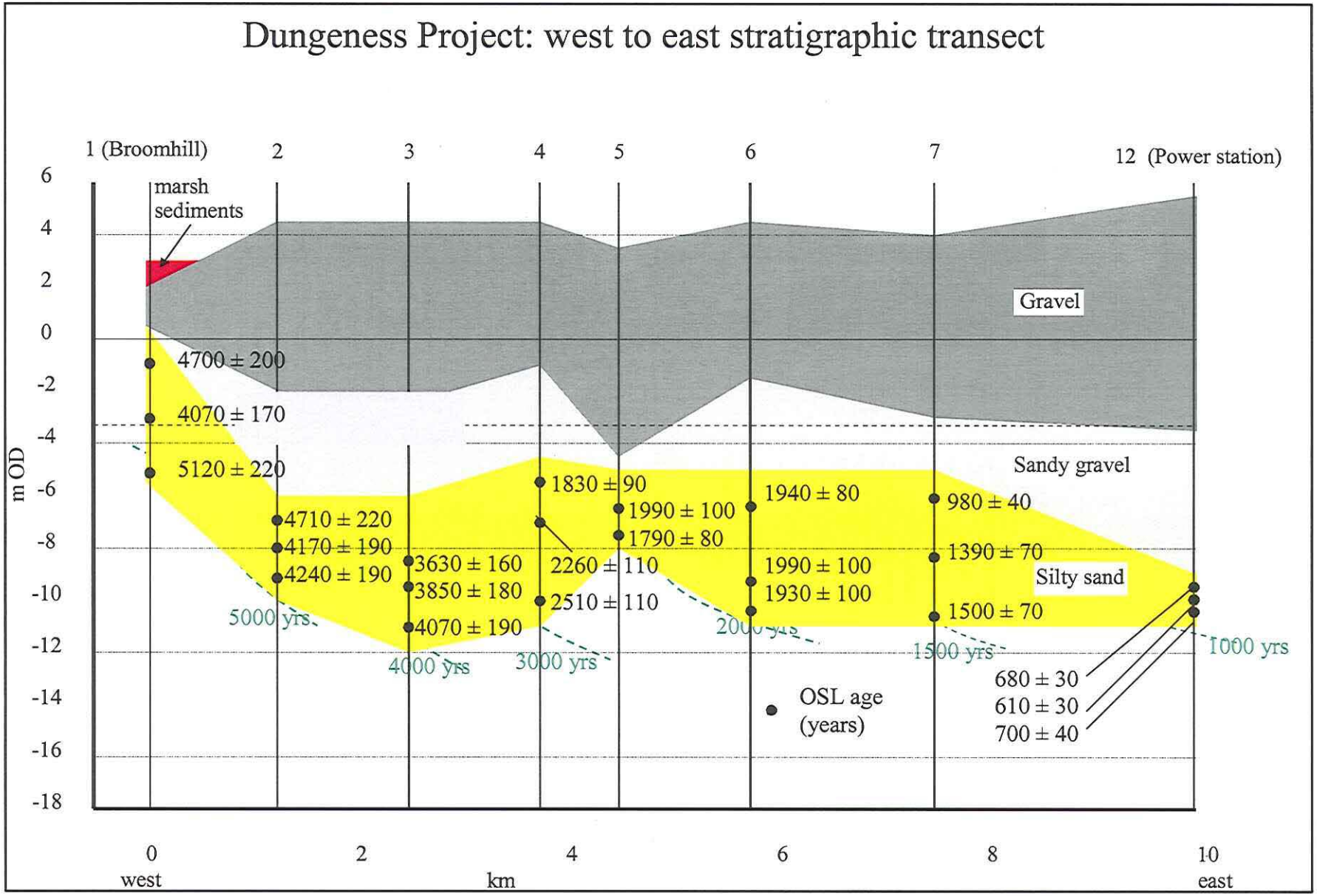

Figure 16a: Hypothetical isochrons (dotted lines) linking OSL ages for samples from the west – east stratigraphic transect across the Dungeness Foreland.

Figure 16b: Hypothetical isochrons (dotted lines) linking OSL ages for samples from the north-south stratigraphic transect across the Dungeness Foreland.

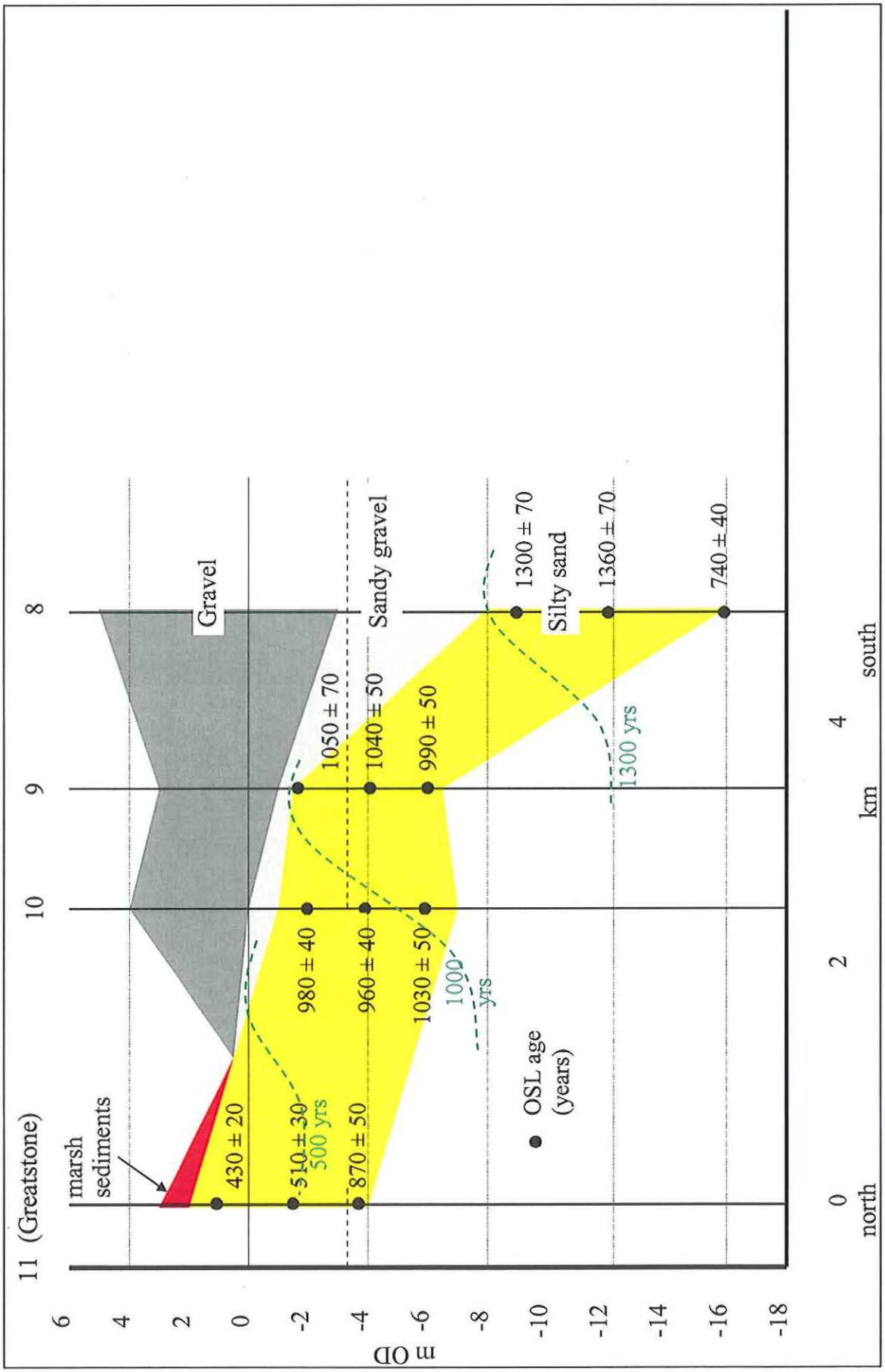

Chronology for Gravel Deposition

When considered in the context of gravel deposition on Dungeness Foreland, the OSL chronology constrains the development of the underlying shoreface sand and tidal flat precursor. In addition, ^{14}C-dated organic deposits in the natural pits on the gravel surface and in the main back-barrier environment (see http://romneymarsh.net/ for regional ^{14}C database) provide minimum ages for gravel beach deposition, ie the gravel substrate was at least in place prior to peat deposition. This approach to obtaining limiting ages may be applied to four sites between Broomhill and Dengemarsh Road, discussed below.

Broomhill Level

For the most westward of the exposed gravel beaches in the region of Broomhill Level, gravel deposition took place between the OSL age range of 5100-4100 years ago for sand accumulation in core 1 and the formation of an overlying peat bed ^{14}C-dated to 1890–1520 cal BC (Tooley and Switsur 1988) (Q-2651: 3410±60 BP). If the youngest OSL age is considered here, the period for gravel formation is further limited to between ~4100 and 3700 years ago.

The Forelands

The OSL age range of ~4100-3600 years ago in core 3 from The Forelands may be linked to a series of ^{14}C-dated inter-ridge peat beds on the adjacent Scotney Marsh site, the oldest of which dates from 2120-1750 cal BC (Spencer *et al* 1998a; 1998b) (Beta-81370: 3580±60 BP).

South Brooks/Wickmaryholm Pit

Here, limiting age data may be established from the OSL age range in core 5 from South Brooks, dating the sub-gravel sands to ~2000-1800 years ago, and the sequence of ^{14}C-dated peat contacts in Wickmaryholm Pit – the oldest of which dates from 370 cal BC-cal AD 140 (Long and Hughes 1995) (UB-3727: 2038±97 BP). Due to potential contamination of this earlier ^{14}C chronology from Wickmaryholm Pit, as evidenced by an age inversion, more recent ^{14}C dating of the sedimentary record has resolved the onset of peat deposition to ~cal AD 250-450 (~1700-1500 cal BP) (Waller *et al* pers comm) (GrA-22407: 1705±30 BP; GrA-22413: 1680±40 BP; OxA-12685: 1652±25 BP), thus limiting the timing of gravel formation to ~1800-1700 years ago at its narrowest window of deposition.

Dengemarsh Road/Muddimore Pit

The recently-established ^{14}C chronology from Muddimore Pit dates the onset of peat formation to ~cal AD 1150-1250 (~800-700 cal BP) (Waller *et al* pers comm) (OxA-12891: 841±31 BP). This may be compared with the OSL age

ranges in core 7 and the uppermost 2 samples of core 8 (discussed in section 8) of ~1500-1000 and ~1300 years ago, respectively. If the uppermost OSL age from the more proximal core site 7 is considered, this gives a more likely temporal window for gravel deposition between 1000 and 800 years ago. This period of gravel beach formation is also likely to pre-date the deposition of marsh sedimentation in the region of Manor Farm where paired valves of *Cerastoderma edule* in rapidly deposited laminated tidal sediments have been dated to cal AD 690-900 (1260-1050 cal BP) (Plater *et al* 2002) (Beta-160061: 1620±40 BP; Beta-160060: 1590±40 BP).

Comparison of OSL and radiocarbon ages in this way is valuable, as together they can constrain the lower and upper units across the foreland, bracketing the time of deposition of the gravel. Additionally, it is worth noting that there are no inconsistencies between the radiocarbon dates and OSL ages.

In addition to the data already discussed, there is some further independent dating evidence which may be considered. The OSL age range in core 4 from Holmstone, giving a period of sub-gravel sand deposition between ~2500 and 1800 years ago, is supported by an earlier well-resolved OSL age from a site a little further north-east beneath the same gravel ridge feature, from a sand lens within the gravel at an altitude of –1.3m OD, giving an OSL age of 1390 ± 80 years ago (Plater *et al* 2002). This single, earlier OSL age dated a period of gravel instability during Anglo-Saxon times. The OSL age for the sands from core 9, ie all ~1000 years ago, may be considered in conjunction with the ^{14}C chronology from the Open Pits in the same area to constrain the time of gravel deposition. However, the peat deposits in this natural pit do show some degree of disturbance where the lowermost contact with an underlying brackish mud can only be dated to 1670-1950 AD (Waller *et al* pers comm) (OxA-12890: 161±30 BP). The OSL ages from core 12 at Dungeness Power Station, which tightly constrain sand deposition to 700-600 years ago, may be compared to ^{14}C-dated shell material in the same sub-gravel sands. The oldest of these ^{14}C ages comes from a 'western' group of boreholes in the region of borehole 12, where the onset of lower sandy facies deposition dates from ~1150 cal BC (~3100 cal BP) (Greensmith and Gutmanis 1990) (HAR-5861: 3140±80 BP). However, the youngest material preserved in the sub-gravel sands comes from shell material at about -34m OD in a borehole to the east of the lighthouse, which is ^{14}C-dated to cal AD 550-780 (1069-735 cal BP) (Beta-27789: 1370±80 BP). As a note of caution, however, in such a high-energy environment there is clearly some concern over reworking of shell material within the sub-gravel sands, meaning that a radiocarbon date obtained from contained shell material may bear an equivocal relationship to the timing of deposition.

Summary for Dungeness Foreland

Although 'paired' OSL and ^{14}C ages have not been obtained from the same cores, ie OSL dating of the sub-gravel sand and ^{14}C dating on above-gravel peat in any given core, the sites from which these limiting ages have been obtained may be linked not only by geographical proximity but also via the established broad-scale pattern of pre- and post-gravel stratigraphy. The chronology of gravel deposition between about 5000 and 1000 years ago is, therefore, now constrained by a suite of consistent and independent age data for the gravel foreland between Broomhill and Denge Marsh. At four sites, in the regions of Broomhill Level, The Forelands, South Brooks, and Dengemarsh Road, the period of gravel deposition quickly follows that of sub-gravel sand body formation, thus supporting the view that the shoreface sand is an essential precursor for, or an integral part of, foreland progradation. Corroboration for the period of foreland progradation after approximately 1000 years ago, or at least for the foreland region east and north-east of Dengemarsh Road, can only be obtained from ^{14}C dates on disturbed or transported biogenic material. However, the gravel in the region of Denge Marsh must have at least been deposited prior to the formation of a widespread sequence of marsh sediments. These have been ^{14}C-dated to 1260-1050 cal years BP (Plater *et al* 2002), and preserve evidence of palaeomagnetic secular variation which dates their rapid deposition to the period of 1200-450 years ago (Plater *et al* forthcoming).

Set within the context of the existing, if discontinuous, chronological model for Dungeness, the OSL chronology provides essential data for the sub-gravel sand body which, in turn, then gives the framework for interpreting the nature and timing of gravel foreland progradation, which may be summarised as follows:

- Sub-gravel sand deposition occurred between about 5000 and 500 years ago in the form of a spit. This was either a precursor to, or an integral part of, foreland progradation.

- Sigmoidal isochrons, interpreted as a sequence of shoreface surfaces, show either an increase in the rate or change in the direction of foreland progradation after about 2000 years ago. The latter is favoured from the observed orientation of successive gravel beach shorelines – suggesting that the present foreland morphology developed to the east of Lydd Beach during the last 2000 years or so. A further increase in rate or change of direction of progradation at ~1300 years ago is equivocal.

- OSL and ^{14}C dating confirms that gravel deposition soon followed progressive development of the sub-gravel sand over the period of ~5000 to 1000 years ago between Broomhill Level and Dengemarsh Road. The period for gravel deposition at four sites between these limits is:
    - Broomhill Level: 4100 to 3700 years ago
    - The Forelands: 4100-3600 to 4000 years ago

- South Brooks: 2000-1800 to 1700 years ago
- Dengemarsh Road: 1000 to 800 years ago

- The OSL chronology for Dungeness Foreland to the east of Dengemarsh Road cannot be fully corroborated, although ^{14}C-dated shell material and a series of PSV ages from overlying marsh sediments on Denge Marsh are supportive of eastward progradation over the period from ~1200-450 years ago.

9.2 Camber Farm

A series of three OSL ages from beneath the gravel ridges in the region of Camber Castle date the accumulation of sub-gravel sand to a period from 940 to 610 years ago. Whilst the oldest of these gives a minimum age for sand accumulation in Rye Bay during the late Holocene, the youngest of these ages dates the transition to gravel beach deposition at Castle Farm to approximately AD 1400. The age is a little older than the AD 1287 date assigned to the gravel fills between Castle Farm and the Daneswall by Lovegrove (1953), but sits well within the AD 1594 shoreline clearly identified from Philip Symonson's map of the district and pre-dates the construction of Camber Castle in AD 1539. Hence, the OSL chronology would appear to provide evidence of sand deposition in the region of Castle Farm prior to the thirteenth-century storms, but the transition to gravel beach formation shortly after. This then dates the north-easterly progradation of the Camber Castle gravel ridge series to a period between AD 1400 and 1594.

9.3 Moneypenny Farm

Sedimentary evidence for landward translocation of the gravel barrier complex during the thirteenth-century storms is sparse in the region of Rye Bay. Investigations around the area of the 'Black Shore' attempted to prove sub-gravel peat deposits following the assumption that the term referred to a post-storm breach shoreline formed where the gravel was swept inland over the back-barrier peat beds. Unfortunately, sub-gravel peats were not located – thus precluding the development of a ^{14}C chronology. However, a sub-gravel sand was proven in the region of Moneypenny Farm. Here, an OSL age of ~ AD 1500 from beneath a *c* 1m thick gravel deposit, pre-dates the deposition of a gravelly-sand then gravel.

The OSL age does not support retreat of the gravel shoreline to the region of Moneypenny Farm following storm breaching of the barrier complex in Rye Bay during the thirteenth-century. However, the evidence here does support inland transport of gravel across an infilled back-barrier drainage network prior to the formation of The Wainway – a significant back-barrier tidal channel that formed after the storm inundation of Rye Bay. This gravel was then redistributed eastward along the northern shore of the Wainway as a series of

small channel margin gravel ridges, as outlined on the soil map of Romney Marsh (Green 1968), which were deposited after AD 1500. This phase of gravel redistribution is corroborated by cartographic evidence, which suggests that the gravel ridge complex was a structural part of the sixteenth- and seventeenth-century reclamation works that took place along the northern bank of the Wainway, and in particular the two embankments constructed near Moneypenny in AD 1532 and 1542 (Eddison pers comm).

10. Summary and Conclusions

The sub-gravel sand unit underlying the Dungeness Foreland and Rye area was dated using OSL applied to coarse-grained quartz. A total of 39 samples were taken for OSL dating, from 12 deep-drill cores running in two perpendicular transects across the Dungeness foreland, plus a deep-drill core at Camber Farm and also a short hand-core at Moneypenny Farm, both in the Rye area. The OSL measurement procedure employed was the Single Aliquot Regenerative dose (SAR) protocol, which corrects for sensitivity change. Several checks and screening criteria were applied to the 1102 OSL dating aliquots and also to additional aliquots prepared from the samples to ensure that the data included in the final age calculation were of the highest quality. The SAR measurement protocol was appropriate for these samples and the sensitivity correction worked well for most aliquots. At higher preheat temperatures, particularly 300°C and 280°C, erroneously high equivalent dose (D_e) values were observed due to thermal transfer of trapped charge; this phenomenon is sometimes a feature of young samples such as those in this study. The samples studied proved sufficiently sensitive and responsive to facilitate well-resolved dating using OSL.

The final OSL ages generated were typically both accurate and of high precision, being supported by other independent dating and cartographic evidence. The uppermost OSL samples from the silty-sand unit dated provide maximum limiting ages for the deposition of the gravel unit that overlies it. These OSL ages showed that the uppermost sub-gravel sands of the Dungeness foreland were deposited between ~4700 and 400 years ago. The OSL ages demonstrated that the foreland developed in an eastwardly direction, with a slight northward depositional trend also being observed in more recent times, suggesting that deposition occurred in almost a spit-like formation. The uppermost samples from the sub-gravel sand units at Camber Farm and Moneypenny Farm also provide maximum limiting ages for the emplacement of the overlying gravel unit, being ~600 years ago and ~500 years ago, respectively.

The spatial distribution of the OSL ages, both laterally and with depth through the Dungeness foreland, permitted the study of deposition and progradation rates of the sub-gravel sand body, which acts as a precursor to gravel deposition and extension of the gravel foreland. Sigmoidal isochrons were plotted, which may approximate former shoreface surfaces as the foreland developed. These isochrons also support the idea of spit-like deposition and elongate foreland development. The isochrons suggest that the progradation rate of the sub-gravel sands increases from around 2000 years ago compared to earlier periods. However, this may simply be an artefact of sampling, with the transect becoming increasingly aligned with the axis of foreland development. Similarly, changes in the deposition rates observed from down-core OSL ages may reflect genuine change in accumulation rates at that particular location, or again, may reflect a change in direction of the feature relative to the sampling transect (ie sampling obliquely versus parallel to the

shoreface). From the observed orientation of successive gravel beach shorelines, a change in direction of the foreland, rather than an increase in the rate of foreland progradation, is favoured as an explanation. The sigmoidal isochrons therefore suggest that the present foreland morphology developed to the east of Lydd Beach during the last ~2000 years. A further increase in rate or change of direction of progradation at ~1300 years ago is equivocal.

Acknowledgements

The cores analysed were sampled by Melvyn and Dean Stupple of Strata Investigation Services, supported by Damien Laidler (University of Durham), Ed Schofield (University of Kingston), and Paul Stupples and Kate Elmore (University of Liverpool). Ed Schofield and Martyn Waller (University of Kingston) sampled the short hand-core from Moneypenny Farm. Paul Stupples is acknowledged for his contribution to the development of the water content history model discussed in section 6 of this report, and kindly thanked for the production of Figures 3-5. Many thanks to Lorraine Morrison (University of Wales, Aberystwyth) for her assistance with chemical preparation of the samples for OSL dating. Geoff Duller (University of Wales, Aberystwyth) is thanked for discussions of the OSL data and for valuable comments on this report. Two anonymous referees are also thanked for their comments on this report. Thanks to all of the project team, particularly the P.I.s from Durham and Kingston, Antony Long and Martyn Waller, and also to Alex Bayliss from English Heritage, for feedback on the OSL ages and discussions of the ages in the context of other data from the area.

References

Adamiec, G and Aitken, M, 1998 Dose-rate conversion factors: update, *Ancient TL* **16**, 37-49.

Aitken, M J, 1985 *Thermoluminescence Dating* London: Academic Press

Aitken, M J, 1994 *Science-based dating in Archaeology*, London: Longman

Aitken, M J, 1998 *An Introduction to Optical Dating*, Oxford: Oxford University Press.

Austin, R M, 1991 Modelling Holocene tides on the NW European Continental shelf, *Terra Nova*, **3**, 276-88.

Bailey, R M, Smith, B W, and Rhodes, E J, 1997 Partial bleaching and the decay form characteristics of quartz OSL, *Radiation Measurements*, **27**, 123 36.

Bailey, S D, Wintle, A G, Duller, G A T, and Bristow, C S, 2001 Sand deposition during the last millennium at Aberffraw, Anglesey, North Wales as determined by OSL dating of quartz, *Quaternary Sci Rev*, **20**, 701-4.

Banerjee, D, Bøtter-Jensen, L, and Murray, A S, 2000 Retrospective dosimetry: estimation of the dose to quartz using the single-aliquot regenerative-dose protocol, *Applied Radiation and Isotopes*, **52**, 831-44.

Barber, L, 1998a An early Romano-British salt-working site at Scotney Court, *Archaeol Cantiana*, **118**, 327-53.

Barber, L, 1998b Medieval rural settlement and economy at Lydd, in J Eddison, M Gardiner, and A Long (eds) *Romney Marsh: Environmental Change and Human Occupation in a Coastal Lowland*, Oxford: Oxford Univ Comm Archaeol Monogr, **46,** 89-108.

Bell, W T, 1979 Attenuation factors for the absorbed radiation dose in quartz inclusions for thermoluminescence dating, *Ancient TL*, **8**, 12-4.

Dix, J, Long, A J, and Cooke, R, 1998 The evolution of Rye Bay and Dungeness Foreland, the offshore seismic record, in J Eddison, M Gardiner, and A Long (eds) *Romney Marsh: Environmental Change and Human Occupation in a Coastal Lowland*, Oxford: Oxford Univ Comm Archaeol Monogr, **46,** 3-12.

Duller, G A T, 2004 Luminescence dating of Quaternary sediments: recent advances, *J Quaternary Sci*, **19**, 183-92.

Eddison, J, 1983 The evolution of the barrier beaches between Fairlight and Hythe, *Geographical J*, **149**, 39-75.

Galbraith, R, 1990 The radial plot: graphical assessment of spread in ages, *Nuclear Tracks and Radiation Measurements*, **17**, 207-14.

Galbraith, R, 2002 A note on the variance of a background-corrected OSL count, *Ancient TL*, **20**, 49-51.

Green, R D, 1968 *Soils of Romney Marsh,* Harpenden: Soil Survey of Great Britain, Bulletin No 4.

Greensmith, J T and Gutmanis, J C, 1990 Aspects of the late Holocene depositional history of the Dungeness area, Kent, *Proc Geologists' Assoc* **101**, 225-37.

Huntley, D J and Lamothe, M, 2001 Ubiquity of anomalous fading in K feldspars and the measurement and correction for it in optical dating, *Canadian J Earth Sci*, **38**, 1093-106.

Lewis, W V, 1932 The formation of Dungeness Foreland, *Geographical J*, **80**, 309-24.

Lewis, W V and Balchin, W G V, 1940 Past sea-levels at Dungeness, *Geographical J*, **96**, 258-85.

Long, A J and Hughes, P D M, 1995 Mid- to late-Holocene evolution of the Dungeness foreland, UK, *Marine Geol*, **124**, 253-71.

Long, A J and Innes, J B, 1995 The back-barrier and barrier depositional history of Romney Marsh, Walland Marsh and Dungeness, Kent, England, *J Quaternary Sci*, **10**, 267-83.

Lovegrove, Capt H, 1953 Old shore lines near Camber Castle, *Geographical J*, **119**, 200-7.

May, V J and Hansom, J D, 2003 *Coastal Geomorphology of Great Britain*, Geological Conservation Review Series, **28**, Joint Nature Conservation Committee, Peterborough.

Mejdahl, V, 1979 Thermoluminescence dating: beta-dose attenuation in quartz grains, *Archaeometry*, **21**, 61-72.

Murray, A S and Wintle, A G, 2000 Luminescence dating of quartz using an improved single-aliquot regenerative-dose protocol, *Radiation Measurements*, **32**, 57-73.

Murray, A S and Wintle, A G, 2003 The single aliquot regenerative dose protocol: potential for improvements in reliability, *Radiation Measurements*, **37**, 377-81.

Needham, S, 1988 A group of Early Bronze Age axes from Lydd, in J Eddison and C Green (eds) *Romney Marsh: evolution, occupation and reclamation*,

Oxford: Oxford Univ Comm Archaeol Monogr, **24**, 77-82.

Olley, J M, Caitcheon, G G, and Roberts, R G, 1999 The origin of dose distributions in fluvial sediments, and the prospect of dating single grains from fluvial deposits using optically stimulated luminescence, *Radiation Measurements*, **30**, 207-17.

Plater, A J, 1992 The late Holocene evolution of Denge Marsh, southeast England: a stratigraphic, sedimentological and micropalaeontological approach, *Holocene*, **2**, 63-70.

Plater, A J and Long, A J, 1995 The morphology and evolution of Denge Beach and Denge Marsh, in J Eddison (ed) Romney Marsh: The Debatable Ground, Oxford: Oxford Univ Comm Archaeol Monogr, **41**, 8-36.

Plater, A, Stupples, P, Roberts, H, and Owen, C, 2002 The evidence for Late Holocene foreland progradation and rapid tidal sedimentation from the barrier and marsh sediments of Romney Marsh and Dungeness: a geomorphological perspective, in A Long, S Hipkin and H Clarke (eds) *Romney Marsh: coastal and landscape change through the Ages*, Oxford: Oxford Univ School Archaeol Monogr Ser, **56**, 40-57.

Plater, A J, Stupples, P, Shaw, J, and Hemetsberger, S, forthcoming Palaeomagnetic Secular Variation (PSV) Dating and Environmental Magnetic Properties of Late Holocene Marsh Sediments, Dungeness, S.E. England, UK, London: English Heritage, *Centre Archaeol Rep* XX/2005.

Prescott, J R and Hutton, J T, 1994 Cosmic ray contributions to dose rates for luminescence and ESR dating: large depths and long-term time variations, *Radiation Measurements*, **23**, 497-500.

Ridgway, J, Andrews, J E, Ellis, S, Horton, B P, Innes, J B, Knox, R W O'B, McArthur, J J, Maher, B A, Metcalfe, S E, Mitlehner, A, Parkes, A, Rees, J G, Samways, G M, and Shennan, I, 2000 Analysis and interpretation of Holocene sedimentary sequences in the Humber Estuary, in I Shennan and J Andrews (eds) *Holocene Land-Ocean Interaction and Environmental Change around the North Sea*, Geological Society of London, Special Pub, **166**, 9-39.

Shennan, I, 1986 Flandrian sea-level changes in the Fenland. II: Tendencies of sea-level movement, altitudinal changes, and local and regional factors, *J Quaternary Sci*, **1**, 155-79.

Shennan, I and Horton, B, 2002 Holocene land- and sea-level changes in Great Britain, *J Quaternary Sci*, **17**, 511-26.

Shennan, I, Lambeck, K, Flather, R, Horton, B, McArthur, J, Innes, J, Lloyd, J, Rutherford, M, and Wingfield, R T R, 2000 Modelling western North Sea palaeogeographies and tidal changes during the Holocene, in I Shennan and J Andrews (eds) *Holocene Land-Ocean Interaction and Environmental Change around the North Sea*, Geological Society of London, Special

Pub, **166**, 299-319.

Spencer, C D, Plater, A J, and Long, A J, 1998a Rapid coastal change during the mid- to late-Holocene: the record of barrier estuary sedimentation in the Romney Marsh region, southeast England, *Holocene*, **8**, 143-63.

Spencer, C D, Plater, A J, and Long, A J, 1998b Holocene barrier estuary evolution: the sedimentary record of the Walland Marsh region, in J Eddison, M Gardiner, and A Long (eds), *Romney Marsh: Environmental Change and Human Occupation in a Coastal Lowland*, Oxford: Oxford Univ Comm Archaeol Monogr, **46,** 13-29.

Spooner, N A, 1994 The anomalous fading of infrared-stimulated luminescence from feldspars, *Radiation Measurements,* **23**, 625-32.

Spooner, N A and Questiaux, D, 1989 Optical dating – Achenhiem Beyond the Eemian using Green and Infrared Stimulation, *Proc of a Workshop on Long and Short Range Limits in Luminescence Dating*, Oxford: RLAHA Occas Pub No 9.

Stokes, S, 1992 Optical dating of young (modern) sediments using quartz: results from a selection of depositional environments, *Quaternary Sci Rev*, **11**, 153-9.

Stokes, S, 1999 Luminescence dating applications in geomorphological research, *Geomorphology*, **29**, 153-71.

Tooley, M J and Switsur, V R, 1988 Water level changes and sedimentation during the Flandrian Age in Romney Marsh area, in J Eddison and C Green (eds) *Romney Marsh: evolution, occupation and reclamation*, Oxford: Oxford Univ Comm Archaeol Monogr, **24**, 53-71.

Wintle, A G and Murray, A S, 2000 Quartz OSL: effects of thermal treatment and their relevance to laboratory dating procedures, *Radiation Measurements*, **32**, 387-400.